

PHENIX Meeting Seminar

Miklos Gyulassy
Columbia University

Oct. 10, 2008
at BNL 2-160

Title:

Non-Mach (anomalous) conical di-jet correlations
associated with future triggered heavy
quark jets as a decisive experimental test
of pQCD wQGP versus AdS/CFT esQGP
dynamical models of the sQGP discovered at RHIC

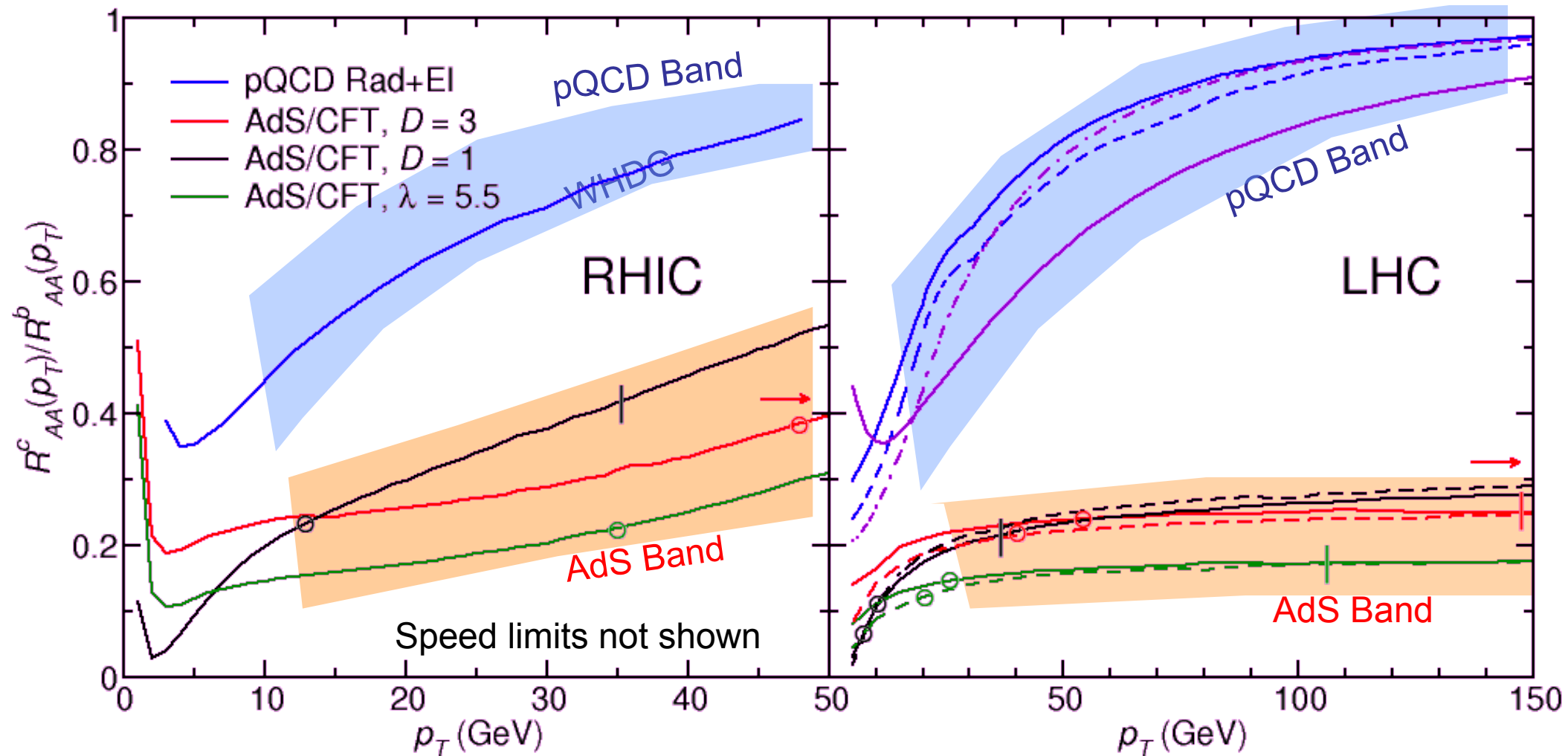
ref: Barbara Betz, Miklos Gyulassy, Jorge Noronha, Giorgio Torrieri
e-Print: [arXiv:0807.4526](https://arxiv.org/abs/0807.4526) [hep-ph]

Experimental Priorities in A+A

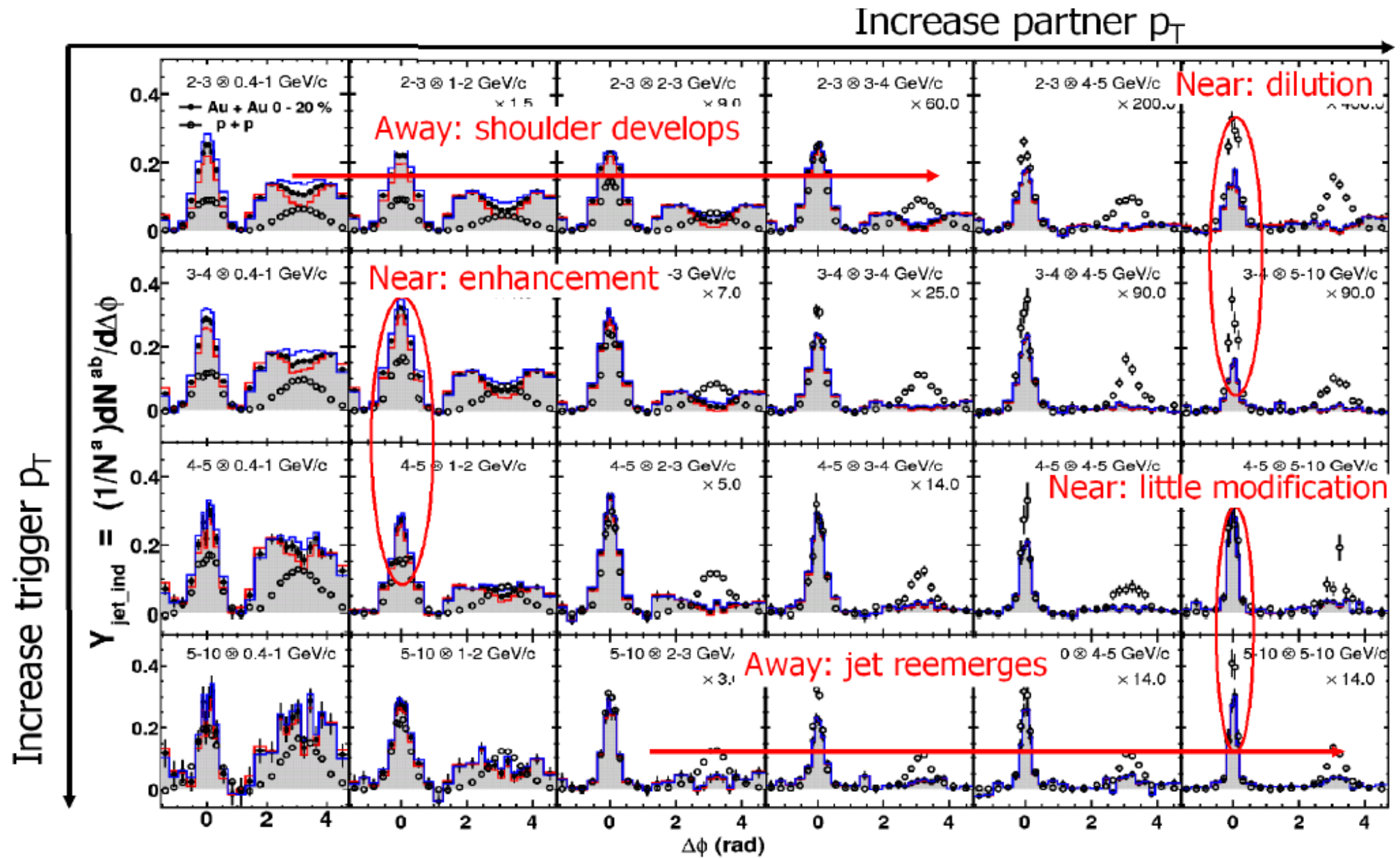
(MG 15.05.2004 @ RBRC Discoveries at RHIC Workshop)

- $Y=0 \pm 3$ test interplay QGP \leftrightarrow CGC ?
- $C_2(\underbrace{\phi_1, \phi_2, p_{t1}, p_{t2}, \eta_1, \eta_2}_{\text{6D microscope}}; \underbrace{f_{l1}, f_{l2}, \text{Mult}, A, B, E_{cm}}_{\text{exp. knobs}})$
- Heavy Quark tomography
- Open Charm (enhancement?); J/Psi (suppression?)
- High pT Charm Flow
- Direct Photons thermometer
- Tagged direct photon -quark jets!
- Turn $E_{cm} \sim 20-200$ and $A=1-100$ exp. knobs

Last year we proposed $R^{cb} = R_{AA}^c(p_T)/R_{AA}^b(p_T)$
as a robust observable to differentiate pQCD vs AdS/CFT
models of sQGP dynamics



Bunching into “pQCD band” vs “AdS/CFT band” is less tight at RHIC
but qualitatively similar to LHC. Note that Lower RHIC T
=> higher AdS speed limits at RHIC though less p_T range accessible than at LHC



MG: We need Triggered Bottom Quark Jet data to navigate correctly through this physics landscape

Correlation data have motivated many diverse theoretical “explanations”

Mach Cones + diffusion wakes + heads + necks are generic supersonic phenomena
and pQCD transport and AdS string drag models both include these basic features.

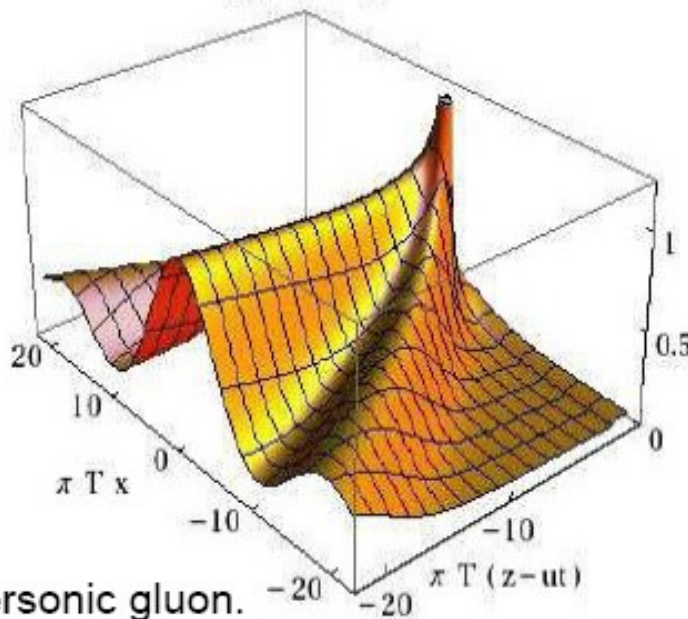
However, the models predict very different observable associated hadron correlations

PQCD

$$\frac{|\vec{x}| g(\vec{x})}{m_D^2 T} \frac{\eta}{s} = 0.13$$

Neufeld et al, 2008

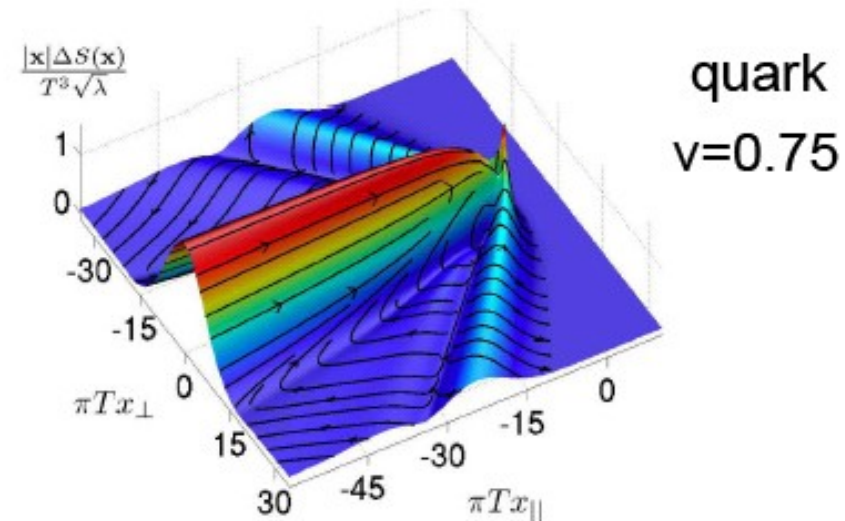
$v=0.999$



Results for a supersonic gluon.
Similar results for quark.

$$\mathcal{N} = 4 \quad \text{SYM}$$

$$N_c \rightarrow \infty \quad \lambda \gg 1$$



P. Chesler, L. Yaffe, 2008.
Similar results also by Gubser et al, 2008.

Anomalous Conical Di-jet Correlations in pQCD vs AdS/CFT

arXiv:0807.4526 [hep-ph]

Barbara Betz^{1,2}, Miklos Gyulassy^{1,3,4}, Jorge Noronha³, and Giorgio Torrieri^{1,4}

Are **Non-Mach** conical correlations in wake of **Heavy Quark** Jet due to **chromo-viscous** hydro coupling effects?

$$\partial_\mu T^{\mu\nu} = \mathcal{S}^\nu = F^{\nu\alpha a} J_\alpha^a = (F^{\nu\alpha a} \sigma_{\alpha\beta\gamma} * F^{\beta\gamma a}) \quad \text{Joule Heating}$$

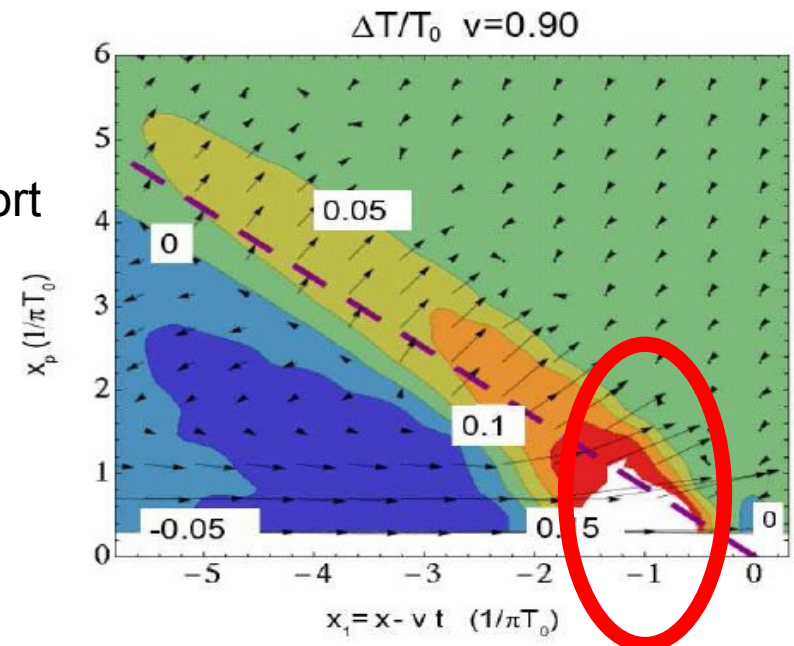
Neufeld(08), Asakawa et al (06) ... Heinz (86)

Color Conductivity Selikhov, MG (93)

$$\sigma_{\mu\alpha\beta}(K) = ig^2 \int d^4P \frac{P_\mu P_\alpha \partial_\beta^P}{P \cdot K + i P \cdot U / \tau^*} f_0(P)$$

The surprise is not that pQCD based chromo transport predicts weak Mach and Diffusion wakes similar to AdS/CFT string drag model predictions,

but that pQCD seems to predict a much weaker nonequilibrium “Neck zone” (within 1fm of the quark) that is the critical source of conical correlations after hadronization.



My Summary:

This may be a smoking gun difference between wQGP pQCD quasiparticle transport and esQGP AdS string drag

What is the physics difference in these models?

In pQCD => Joule heating in the near ($r < 1$ fm) “Neck zone”

The very strong “Red Neck” physics predicted by AdS/CFT is still a mystery

Future identified heavy quark jet tomography will be decisive to judge between

Is the sQGP = $\lim_{\alpha \rightarrow 0.5}$ pQCD/wQGP ?

Is the sQGP = $\lim_{0.5 \leftarrow \alpha = \lambda/12\pi}$ BH/AdS drag ?

or something else ???

Gyulassy 10/10/08 BNL

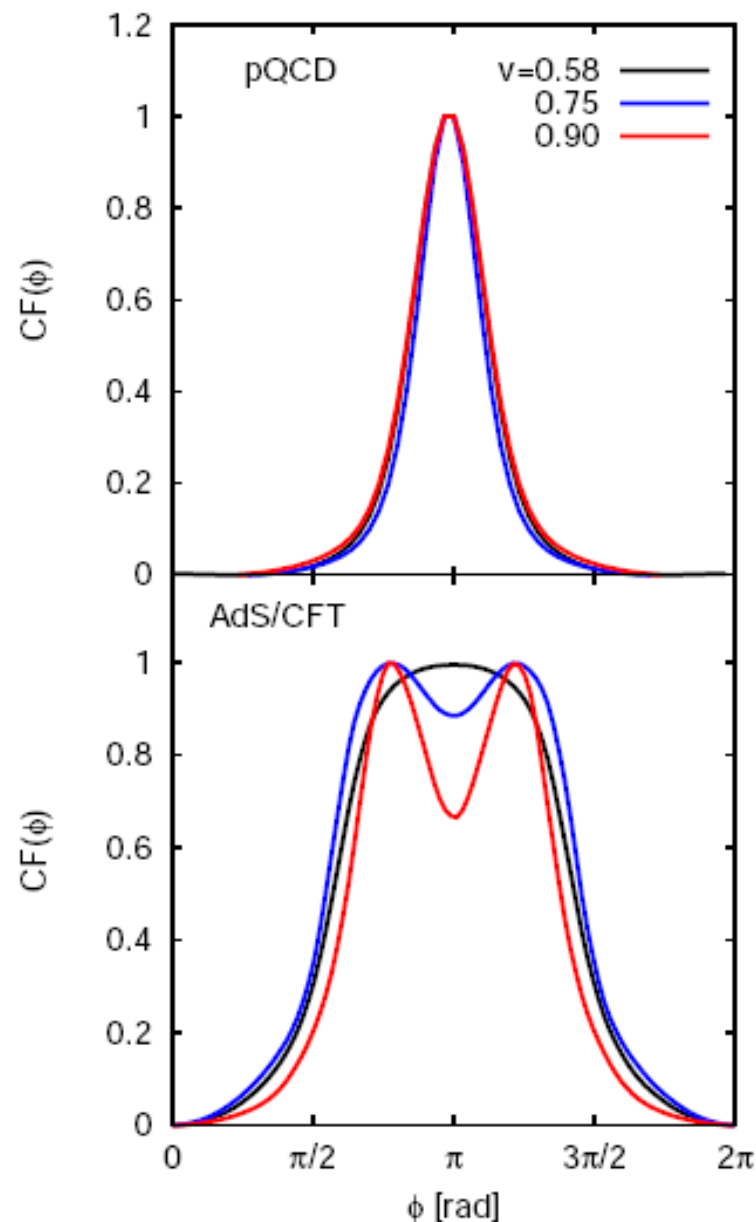
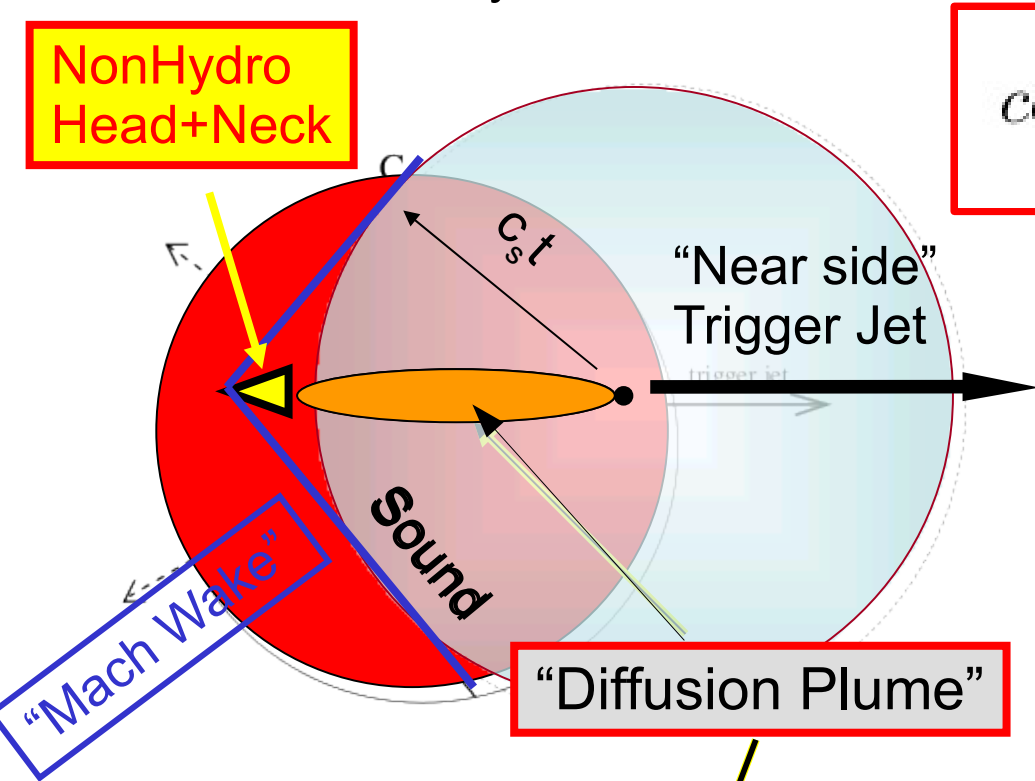


FIG. 4: (Color online) Normalized (and background subtracted) azimuthal away side jet associated correlation after Cooper-Frye freeze-out $CF(\phi)$ (see Eq. 15) for pQCD (top) and AdS/CFT from [5] (bottom). Here $CF(\phi)$ is evaluated at $p_T = 12.5 T_0 = 2.5$ GeV and $y = 0$. The black line is

F. Antinori, E.V. Shuryak, 2005.



$$\cos\theta_M = \frac{\bar{c}_s}{v_{jet}}$$

“Mach's Law”

Problem is how to calibrate this “Barometric” Observable?

Observed Angular and spectral distribution

Is a superposition of many components:

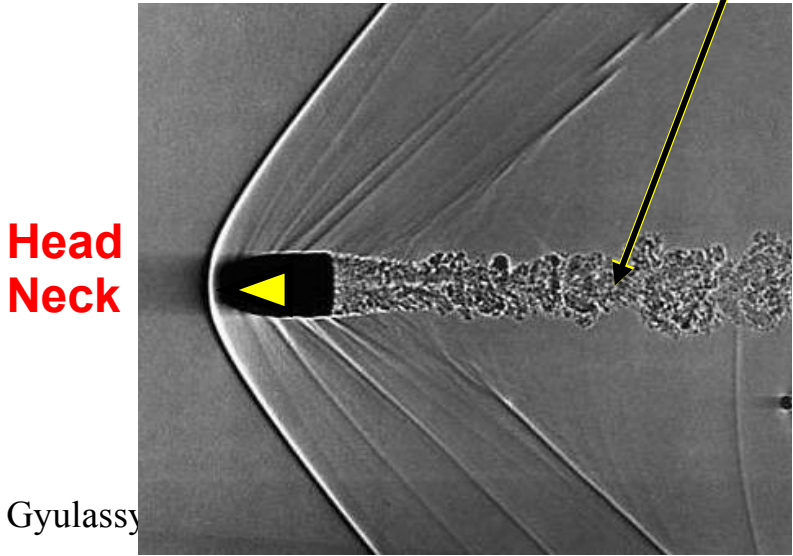
$$dN/d\eta dp_T d\phi = \text{Mach wake} + \text{Diffusion Plume} + \text{Flowing Bulk sQGP}$$

Casaderrey-Solana, et al 06

 + Jet Head + Neck

J.Noronha, B. Betz, G. Torrieri, MG (08)

Unlike a supersonic bullet, a Heavy Quark produces a fragmented near zone head and neck source of correlations the dominate the final hadron signal!!



Ideal "Mach's Law"

$$\cos\theta_M = \frac{\bar{c}_s}{v_{jet}}$$

Only applies (*in the ideal homogeneous static plasma case*)
to only one of the four distinct stress zones in the wake of a supersonic Quakk

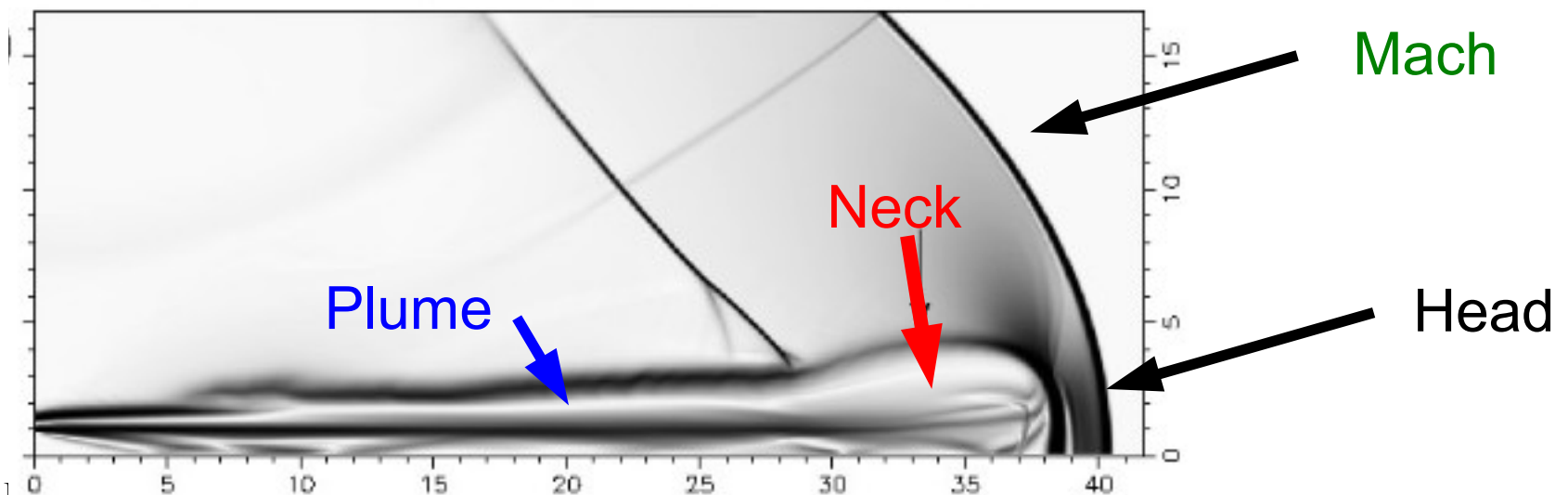
1. Mach Zone $r > 1 \text{ fm}$ $z < 0$

2. Shear Plume $r < 1 \text{ fm}$ $z < -1 \text{ fm}$ (Diffusion wake)

3 Neck Zone $r < 1$ and $|z| < 1$

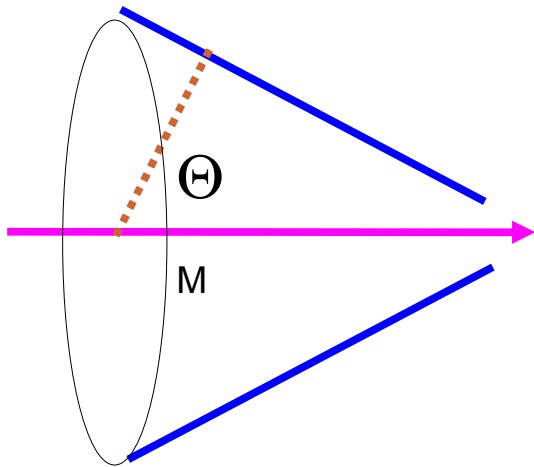
4 Coulomb head $r < 1/\sqrt{\gamma}$ and $|z| < 1/\sqrt{\gamma^3}$

Non-Mach
sources of
Correlations

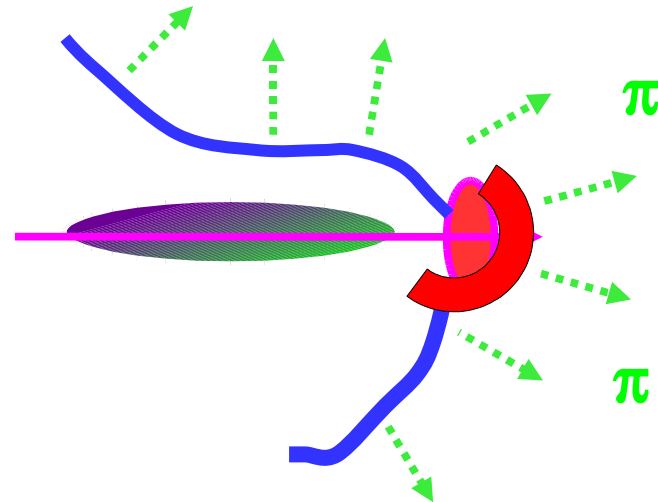


Here we neglect Many Distortions of Ideal Conical Correlations in A+A
to clarify pQCD vs AdS physics differences

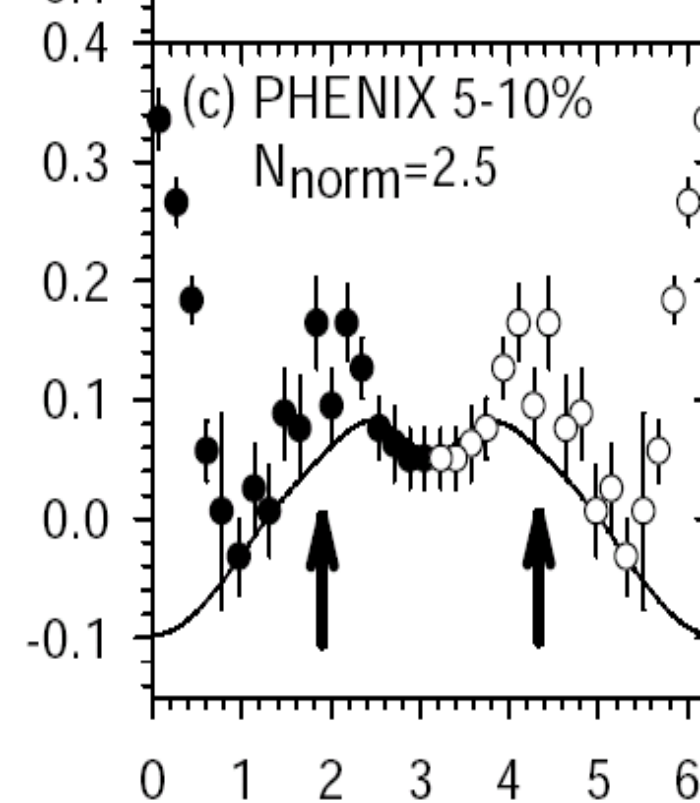
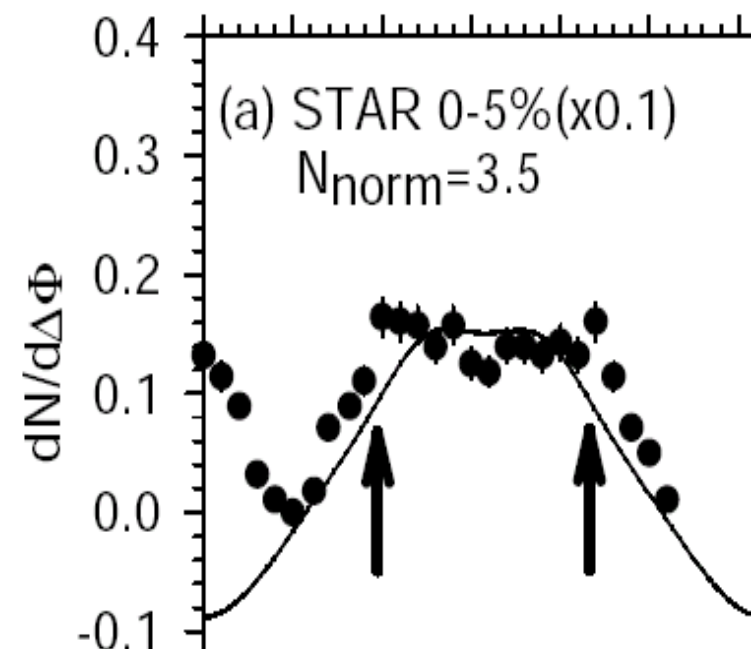
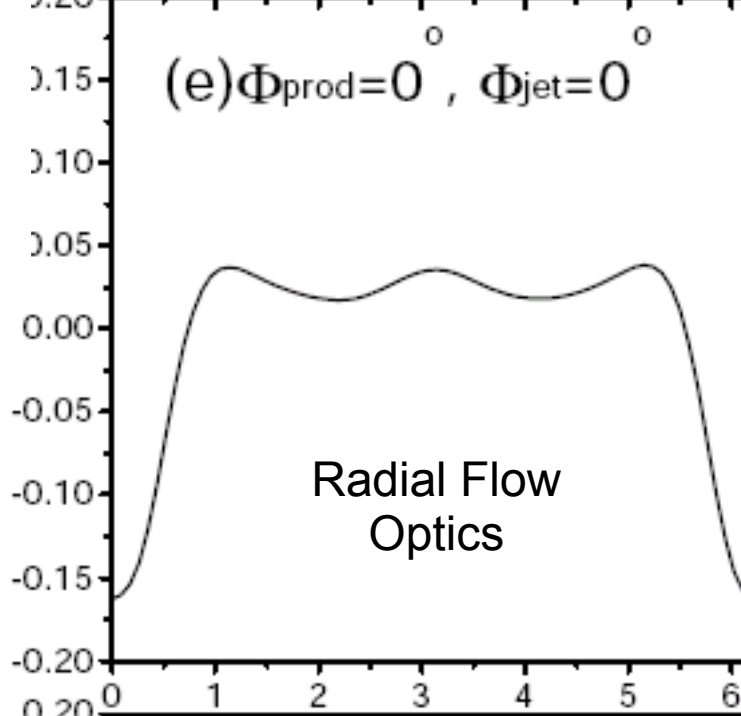
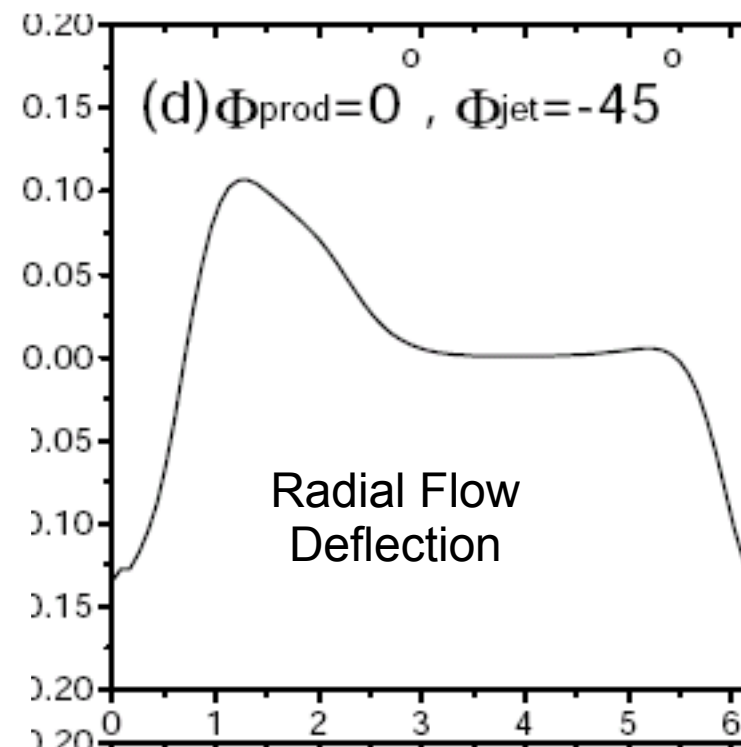
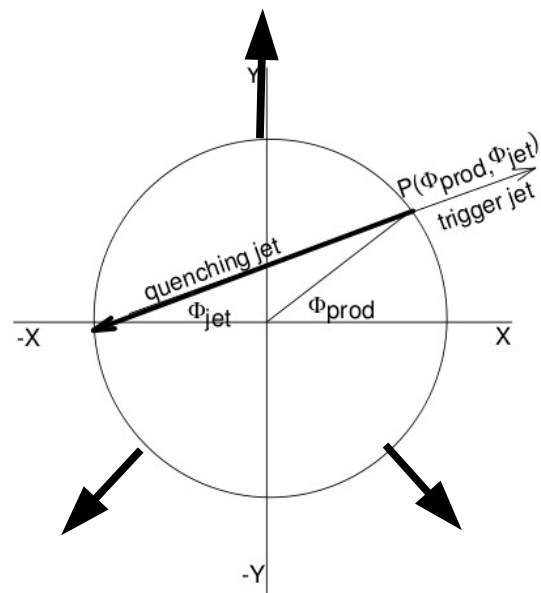
- 1) Geometric $\mathbf{x}_{\text{jet}}(\tau)$: variations of jet trajectory through the QGP $\rho(\mathbf{x}, \tau)$
- 2) Radial, Elliptic Flow, and Longitudinal of QGP
- 3) Local Equation of State $T(\mathbf{x}, \tau) \Rightarrow \cos \Theta_M(\tau) = v_s(\mathbf{x}_{\text{jet}}(\tau), \tau) / c$
- 4) Hadronization (Cooper-Frye+Coalescence+pQCD fragmentations)



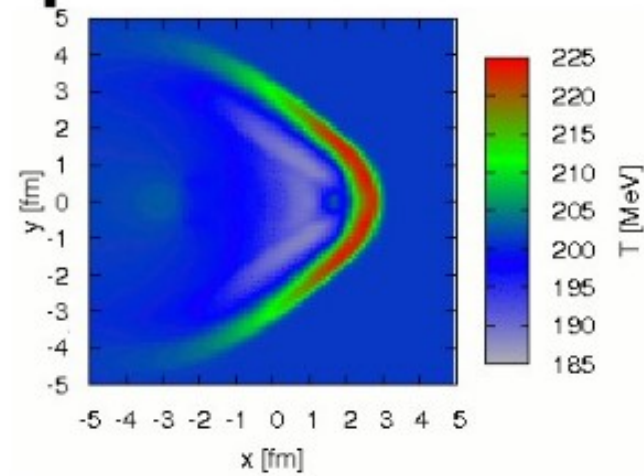
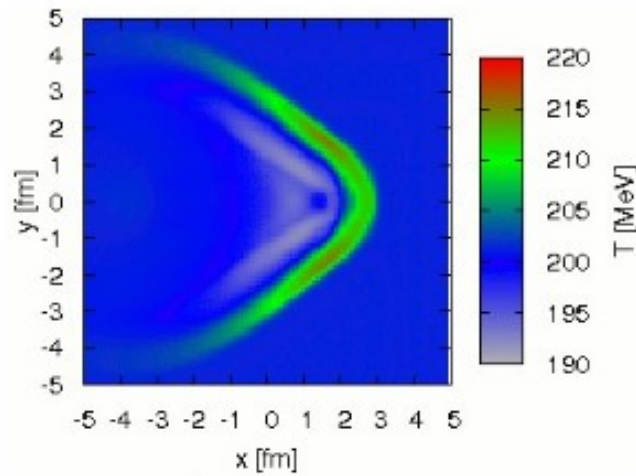
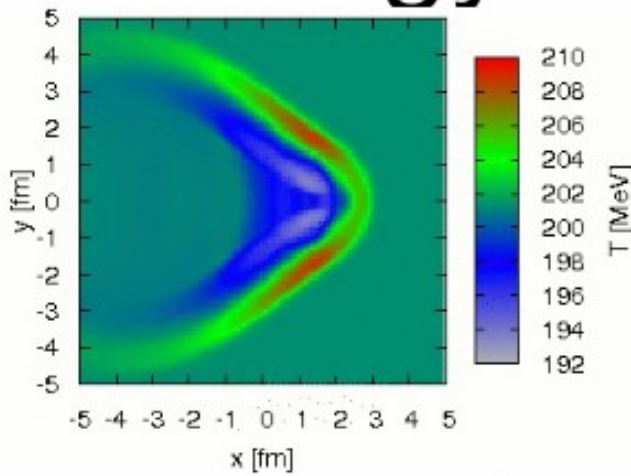
Ideal Mach cone



Distorted Machs in A+A
plus distorted plume+head+neck+... ¹⁰



Energy & Momentum Deposition

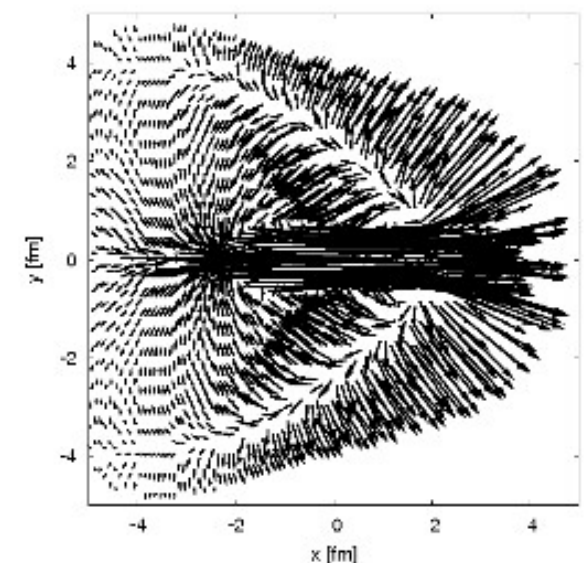
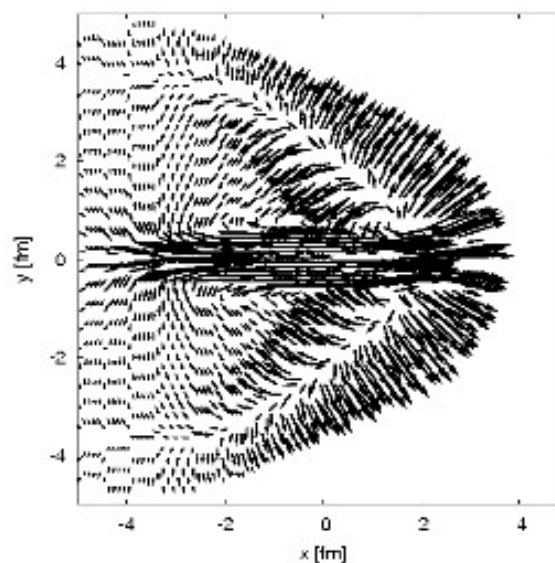
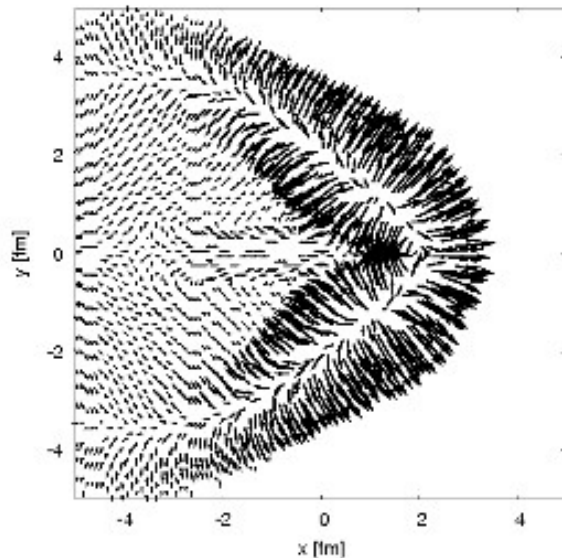


$$\frac{M_{\text{jet}}}{E_{\text{jet}}} = 0$$

$$\frac{dE}{dx} = 1.4 \frac{\text{GeV}}{\text{fm}}$$

$$\frac{M_{\text{jet}}}{E_{\text{jet}}} = \frac{1}{2}$$

$$\frac{M_{\text{jet}}}{E_{\text{jet}}} = 1$$

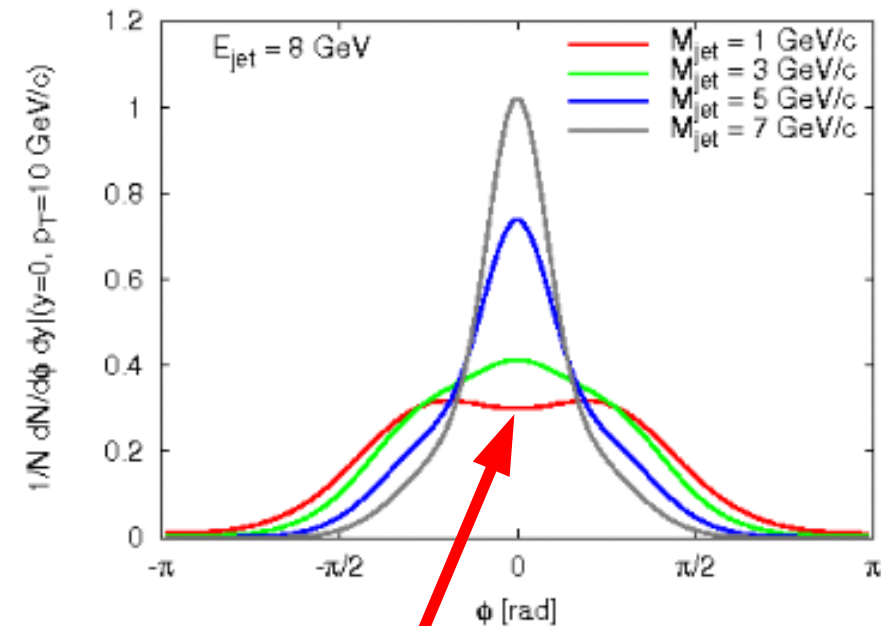
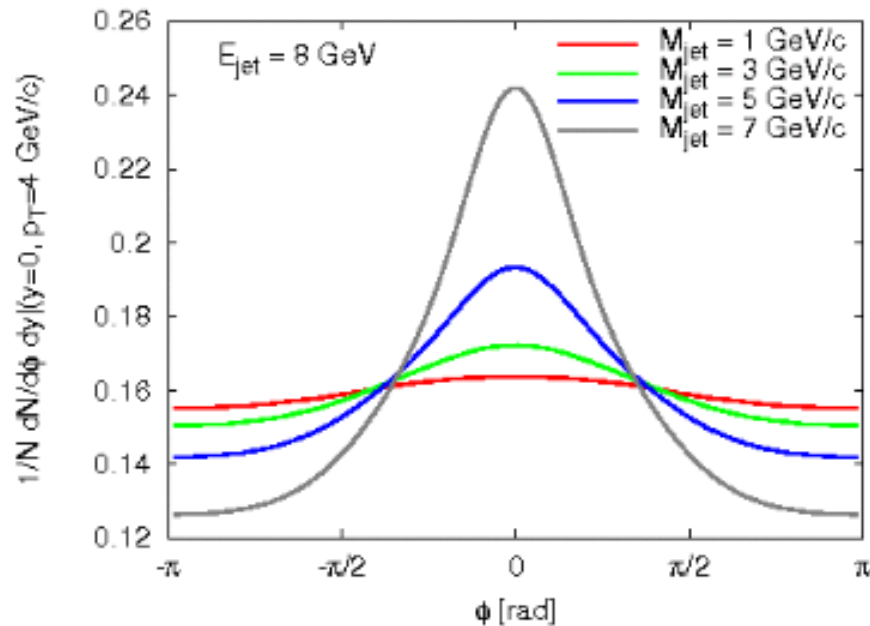


Cooper-Frye Hadronization of 3+1 D Relativistic Hydrodynamics

$dE/dx = 1.4 \text{ GeV/fm}$, $L = 5 \text{ fm}$, with different dP/dx : $dP / dE = 1/8, 3/8, 5/8, 7/8$

$p_T = 4 \text{ GeV}$

extreme $p_T = 10 \text{ GeV}$



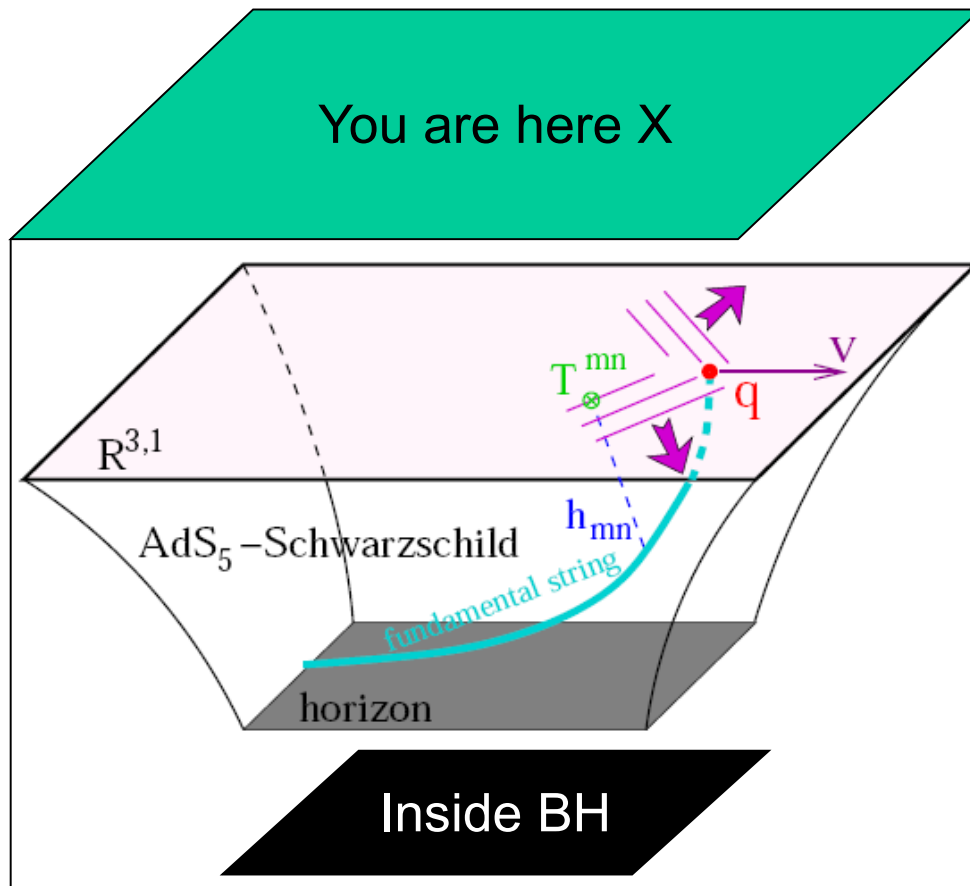
Dip only appears for
unphysical small dP / dE
and unphysical large p_T

Huge forward “shear plume” fills conical dip if $dP > 0.2 dE$

Consistent with Casadelrey-Solana et al using linearized Navier Stokes

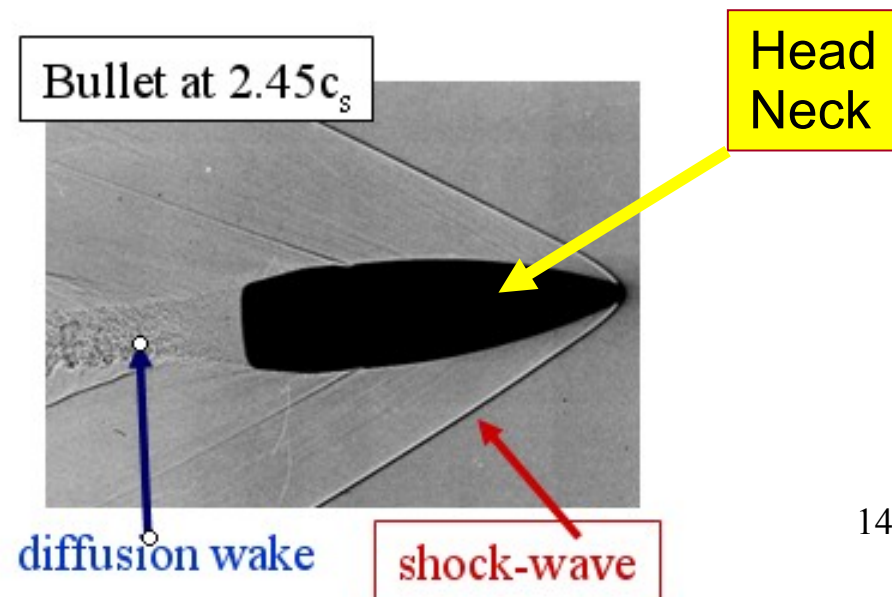
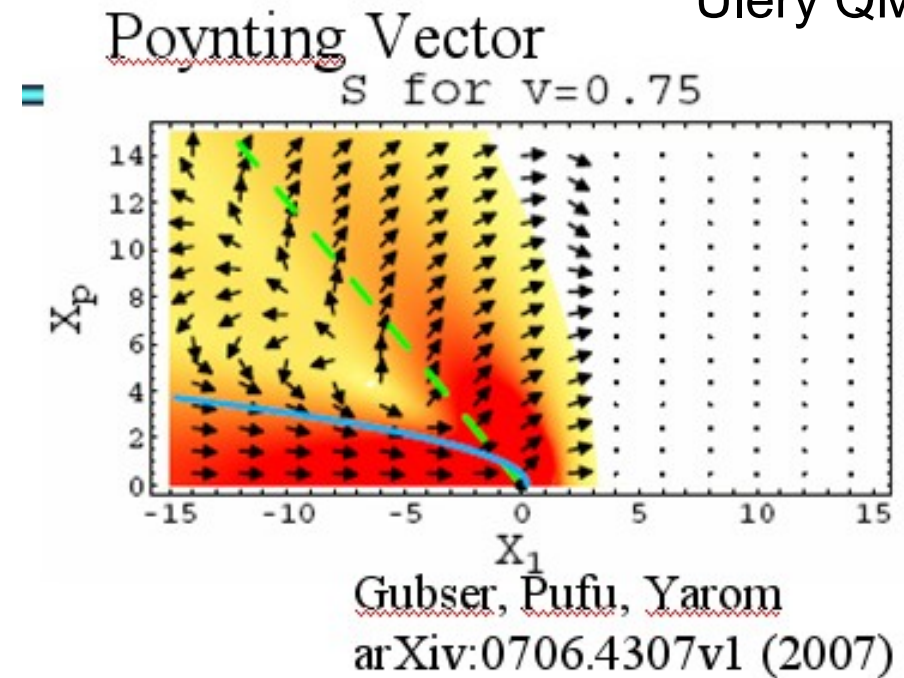
Jet Induced Mach Cones in SYM Plasmas via the AdS/CFT Heavy Quark String Drag Model

Ulery QM08



2006-
Herzog et al
Gubser et al
Yaffe et al

Similar to Bullet
but AdS stress
in the head and neck
is "soft"

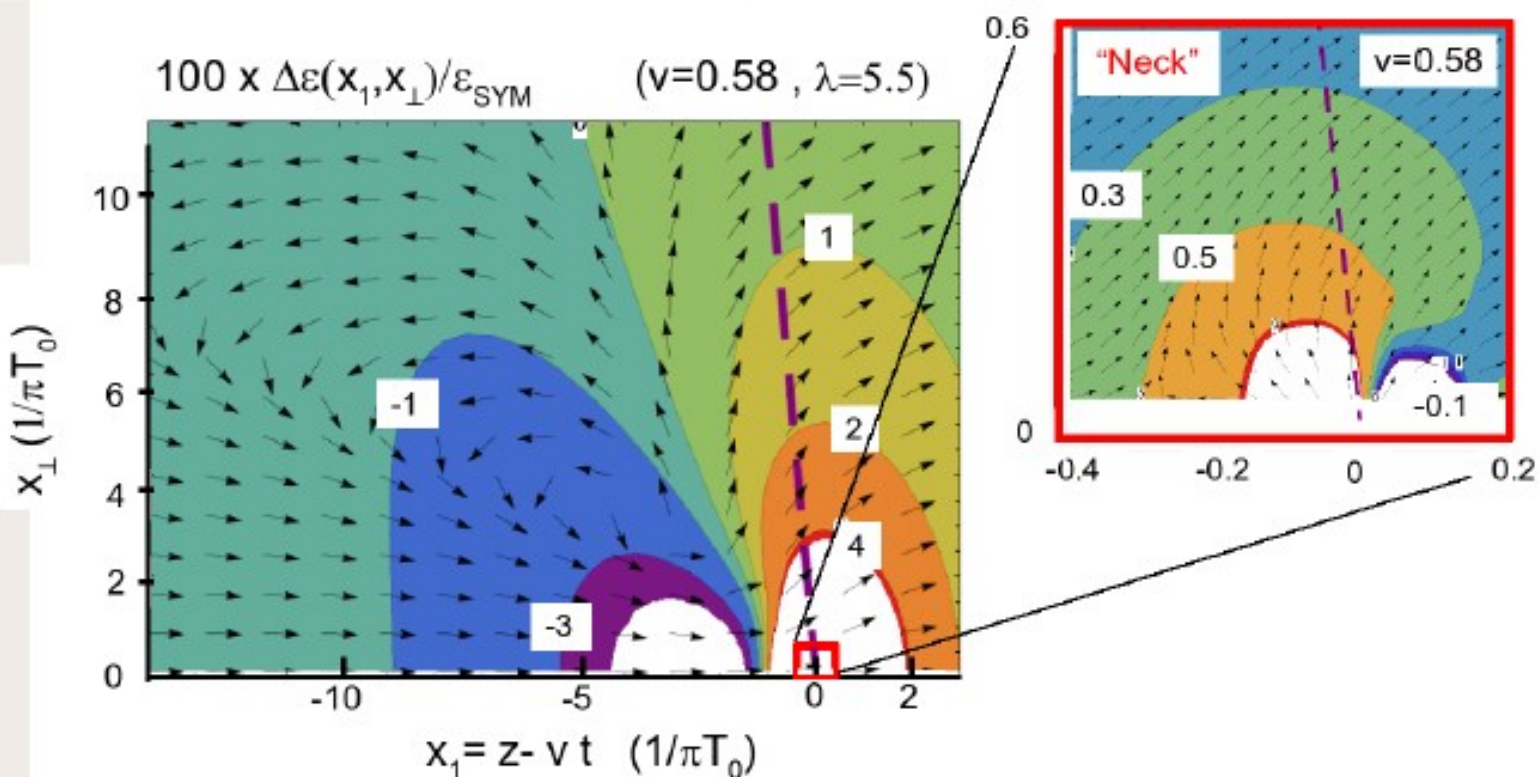
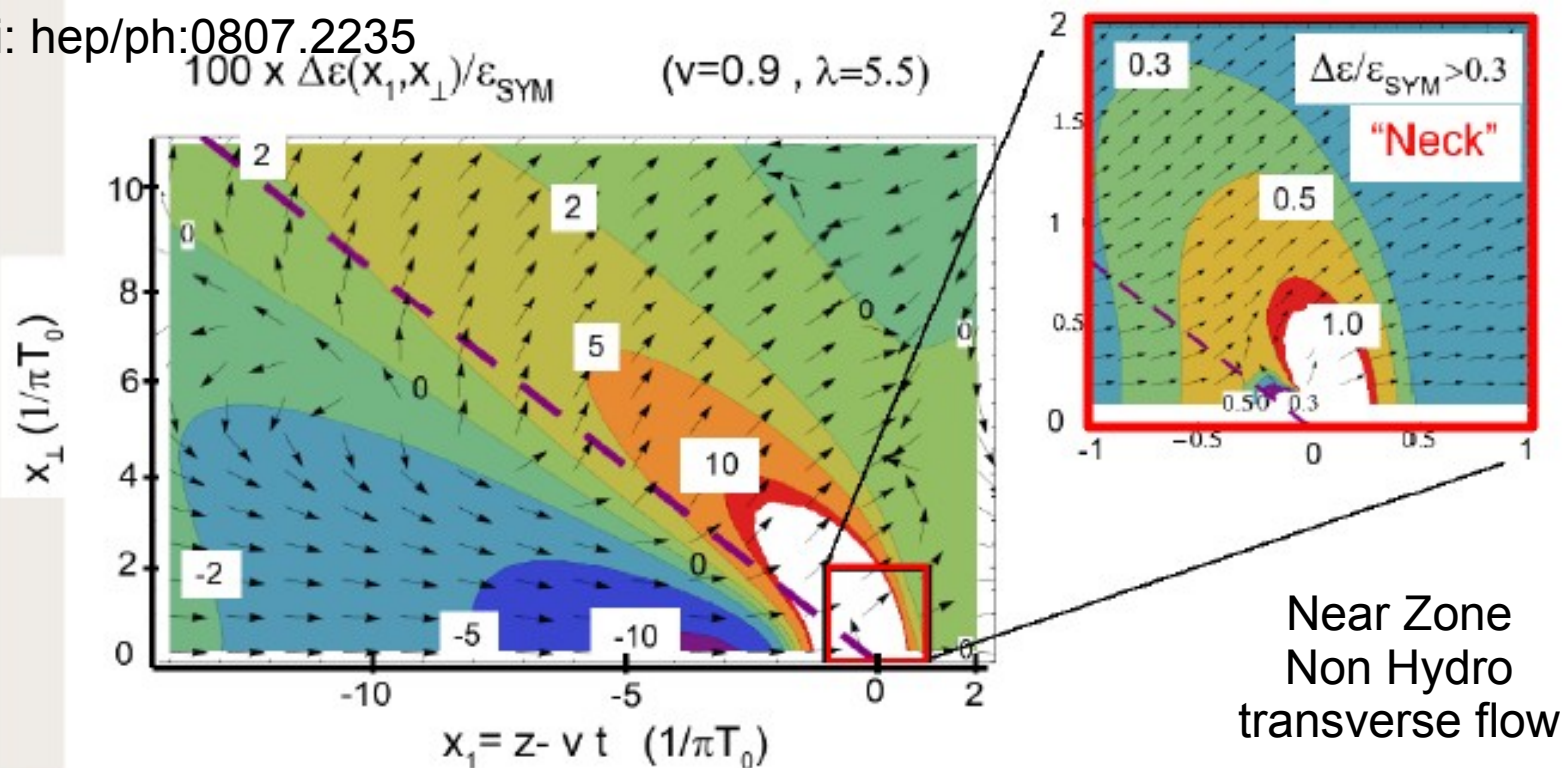


Gubser et al 2007
AdS String Drag
Stress “Holograms”

$v=0.90\ c$
 $p_b=9.3\ \text{GeV}$

$c_s=0.5774\ c$

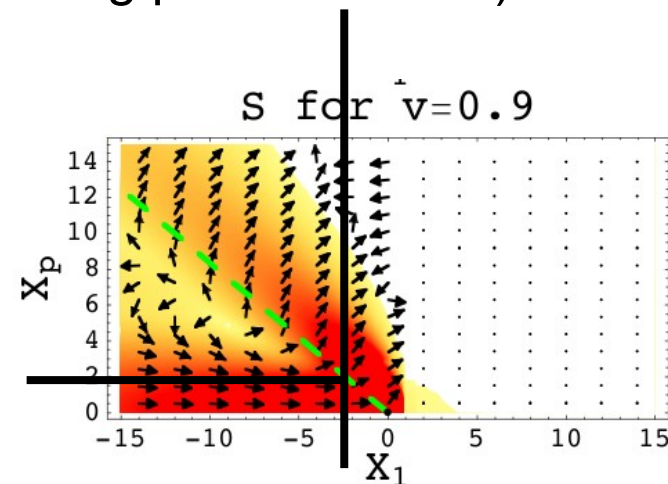
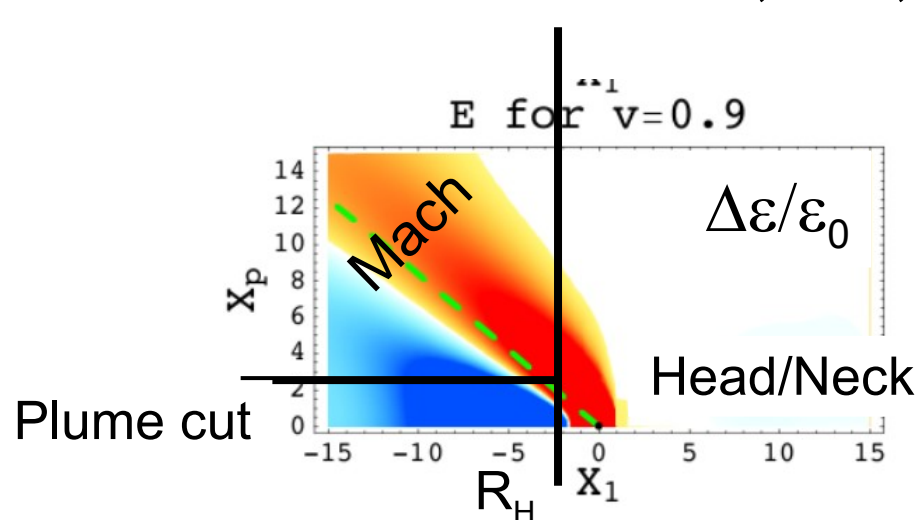
$v=0.58\ c$
 $p_b=3.2\ \text{GeV}$



Cooper-Frye hadronization of AdS or QCD $T^{\mu\nu}(x)$ stress “data”

$$(T(x), \vec{v}(x)) \xrightarrow{\text{Cooper-Frye}} dN^m / d^3p$$

AdS stress of Gubser, Pufu, Yarom (<http://arxiv.org/pdf/0706.4307>)



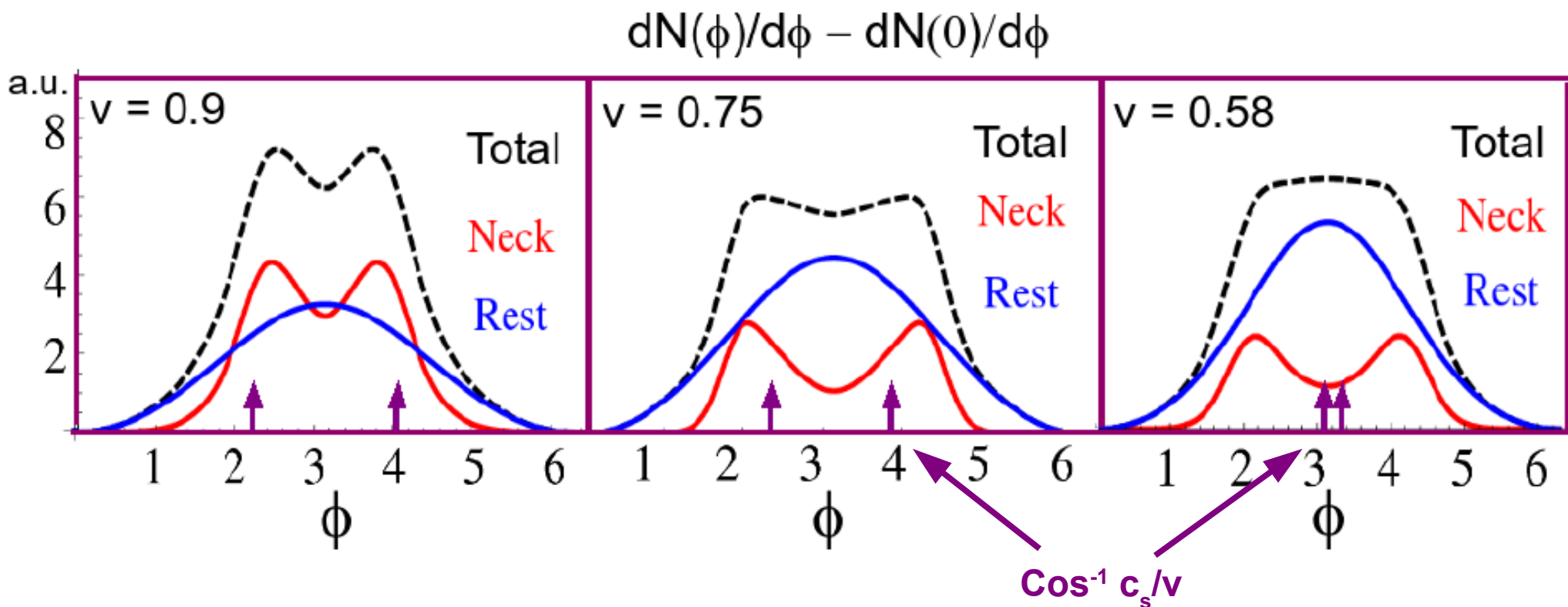
$$\frac{dN}{d\varphi dy} \Big|_{y=0} = \frac{g}{(2\pi)^3} \int dV \int dp_{\perp} \sqrt{p_{\perp}^2 + m^2} p_{\perp} \exp \left\{ -\frac{\gamma}{T} \left[\sqrt{p_{\perp}^2 + m^2} - p_{\perp} (v_x \cos \varphi + v_y \sin \varphi) \right] \right\}$$

AdS (T, v) assumes static SYM plasma. so we use [isochronous freeze-out](#)

Cooper-Frye Hadronization of Gubser et al AdS Drag Solution

The far zone is dominated by the diffusion plume away side peak at $\phi=\pi$

But near zone Neck stress has a strong transverse flow that leads to Conical correlations that do not obey Mach's law !!



quark jet velocity and associated hadron transverse momentum ranges, 1 : ($v/c = 0.9, p_T/\pi T_0 = 4-5$), 2 : ($v/c = 0.75, p_T/\pi T_0 = 5-6$), and 3 : ($v/c = 0.58, p_T/\pi T_0 = 6-7$), are compared. The short arrows show the expected Mach angles.

$f(\phi) = dN/p_T dp_T dy d\phi|_{y=0}$ with respect to the nuclear beam axis is then given after integrating over φ by

$$f(\phi) = 2\pi p_T \int_{\Sigma_T} dx_1 dx_\perp x_\perp \times \quad (4)$$

Cooper-Frye

$$\left(\exp \left\{ -\frac{p_T}{T} [U_0 - U_1 \cos(\pi - \phi)] \right\} I_0(a_\perp) - e^{-p_T/T_0} \right)$$

where $a_\perp = p_\perp U_\perp \sin(\pi - \phi)/T$ and I_0 is the modified Bessel function. In the supergravity approximation $a_\perp \sim \mathcal{O}\left(\frac{\sqrt{\lambda}}{N_c^2}\right) \ll 1$ and, thus, we can use the expansion for the Bessel function

$$\lim_{x \rightarrow 0} I_0(x) = 1 + \frac{x^2}{4} + \mathcal{O}(x^4) \quad (5)$$

to get the approximate equation for the distribution

$$f(\phi) \simeq e^{-p_T/T_0} \frac{2\pi p_T^2}{T_0} \left[\frac{\langle \Delta T \rangle}{T_0} + \langle U_1 \rangle \cos(\pi - \phi) \right] \quad (6)$$

Broad Recoil Blob
(Borghini 2004)

deviations from isotropy are then controlled by the following global moments $\langle \Delta T \rangle = \int_{\Sigma_T} dx_1 dx_\perp x_\perp \Delta T$ and $\langle U_1 \rangle = \int_{\Sigma_T} dx_1 dx_\perp x_\perp U_1$.

Why do far zone
Mach wakes
leave no
conical signature ?

Because
they are
weak sound
waves

Why are Mach Cones in infinitely coupled SYM are so weak ?

Linearized Navier-Stokes hydrodynamics provides a good description of the heavy quark's wake down to distance scales of $1/T_0$ away from the heavy quark.

$$N_c \rightarrow \infty \quad \lambda \gg 1$$

Noronha, Torrieri, Gyulassy, PRC 78, 024903 (2008).
Chesler, Yaffe, PRC 78, 045013 (2008).

How big are the flow and temperature fluctuations created by the heavy quark?

Flow

$$U^\mu = (\sqrt{1 + \vec{U}^2}, \vec{U}) \quad \text{One can show that}$$

$$U^i = \frac{T^{0i}}{4p_0} \sim \mathcal{O}(\sqrt{\lambda}/N_c^2)$$

We obtain that the local temp.

$$T(X) = T_0 + \Delta T(X)$$

$$\Delta T(X)/T_0 \sim \mathcal{O}(\sqrt{\lambda}/N_c^2)$$

The supergravity approximation is only valid when $g_{\text{YM}} \rightarrow 0$ but $N_c \rightarrow \infty$ such that $\lambda \rightarrow \infty$ and $\sqrt{\lambda}/N_c^2 \rightarrow 0$!

Very strong stress structure
is however predicted in
sub thermal $r < 1/3T$
near zone

$\Delta\epsilon/\epsilon \sim 1$ and transverse flow

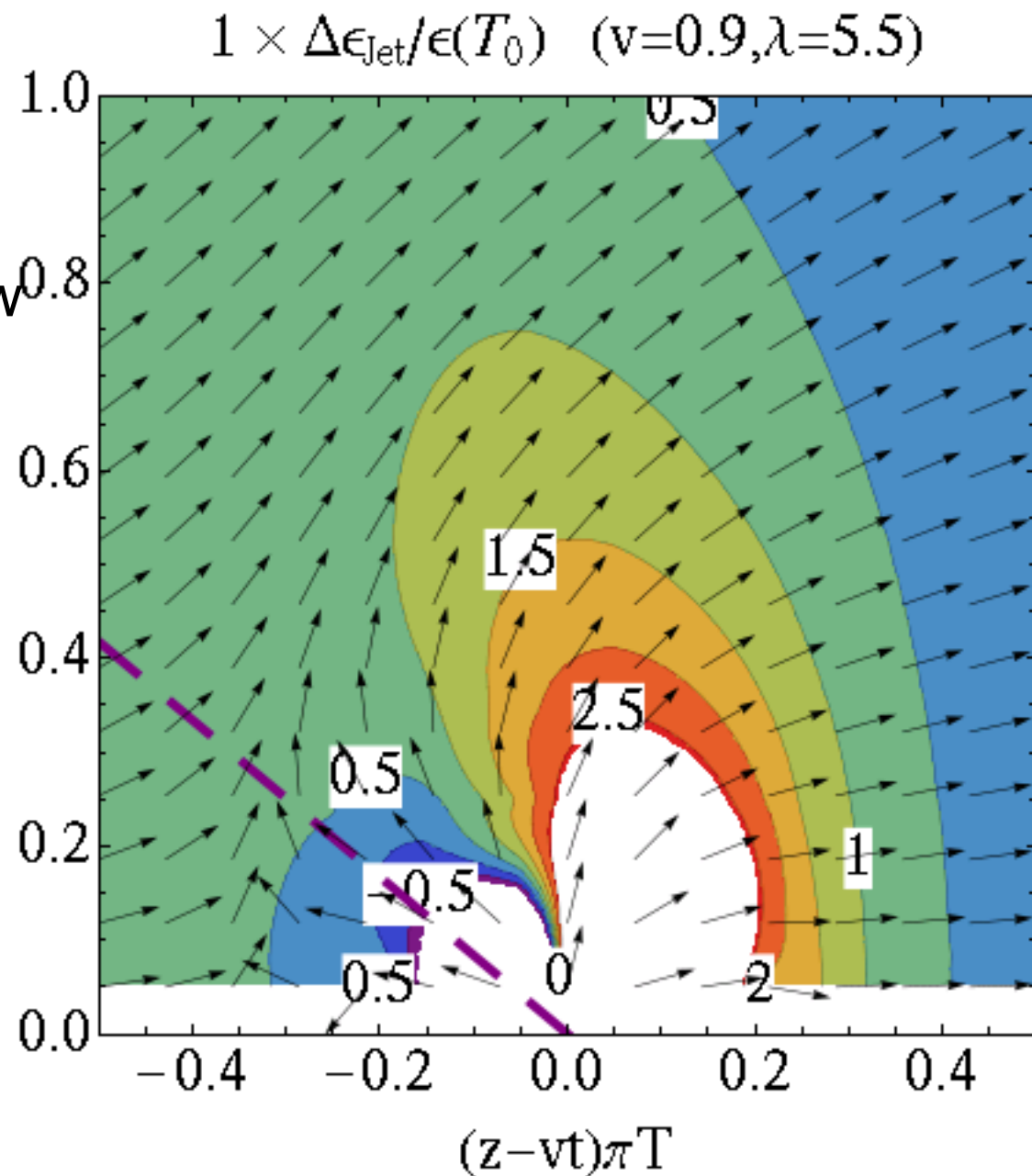
induced in AdS
response to passing
heavy quark with $v=0.9$

even in the **top down**
“weak” coupling extrapolation

$N_c = 3 \ll \infty$

$\lambda = g_{\text{YM}}^2 N_c = 5.5 \ll \infty$
($\alpha=0.15$)

needed for AdS to be consistent
with lattice QCD



GPY07 numerical stress data

Part II: pQCD based Chromo-Hydrodynamic sources of conical correlations

Is the AdS Neck Conical correlation source universal or is it a unique signature of very strongly coupled plasma dynamics?

Can we use pQCD to identify the non-equilibrium physics in the neck?

- > **Quark - Gluon Transport Theory. Part 2. Color Response And Color Correlations In A Quark - Gluon Plasma.**
[Ulrich W. Heinz](#) ([Brookhaven](#)) . BNL-36721, (Received Jul 1985). 55pp.
Published in **Annals Phys.****168:148,1986**.
- > **Color diffusion and conductivity in a quark - gluon plasma.**
[Alexei Selikhov](#), [Miklos Gyulassy](#) ([Columbia U.](#)) . CU-TP-598A, Jun 1993.
Published in **Phys.Lett.****B316:373-380,1993**.
- > **Anomalous transport processes in anisotropically expanding quark-gluon plasmas.**
[Masayuki Asakawa](#) ([Osaka U.](#)) , [Steffen A. Bass](#) ([Duke U.](#)) , [Berndt Muller](#) ([Duke U.](#) & [Kyoto U.](#), [Yukawa Inst., Kyoto](#)) . Aug 2006. 31pp.
Published in **Prog.Theor.Phys.****116:725-755,2007**.
- > **Sonic Mach Cones Induced by Fast Partons in a Perturbative Quark-Gluon Plasma.**
[R.B. Neufeld](#), [Berndt Muller](#) ([Duke U.](#)) , [J. Ruppert](#) ([Frankfurt U.](#) & [McGill U.](#)) . Feb 2008. 5pp.
e-Print: **arXiv:0802.2254** [hep-ph]

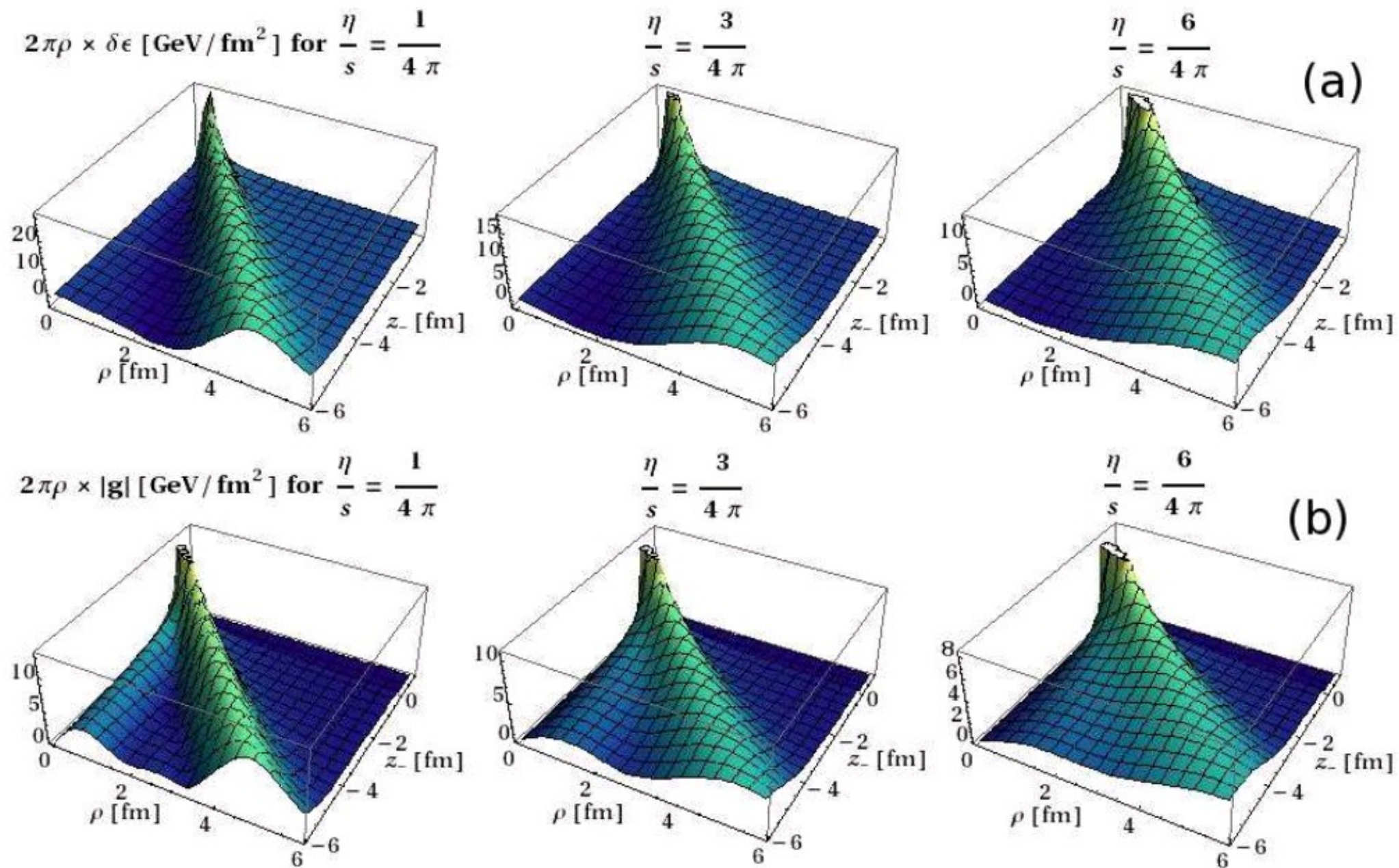
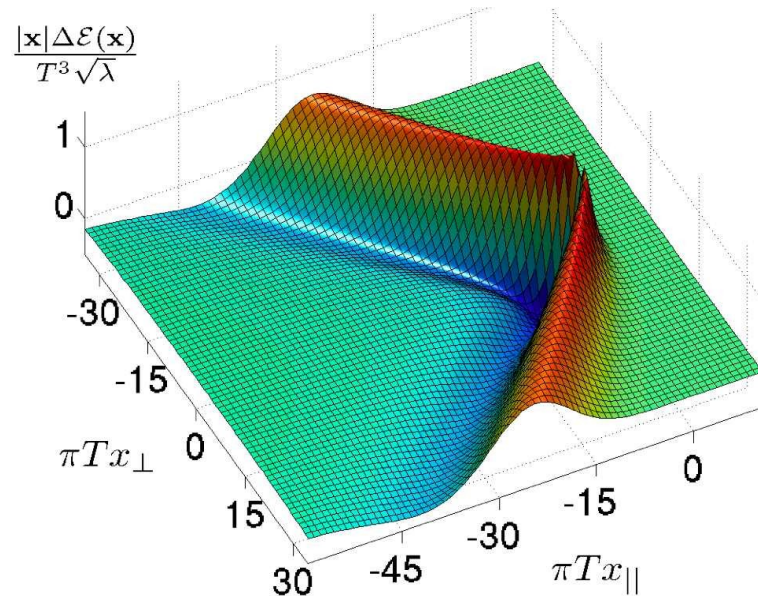


FIG. 5: (Color online) Plots of (a): the total perturbed energy density, and (b): the total perturbed momentum density, contained at a given radius in the $\rho - z_-$ plane. As one can see in (b) the total perturbed momentum density carried by the sonic Mach cone exceeds that contained in the diffusive wake

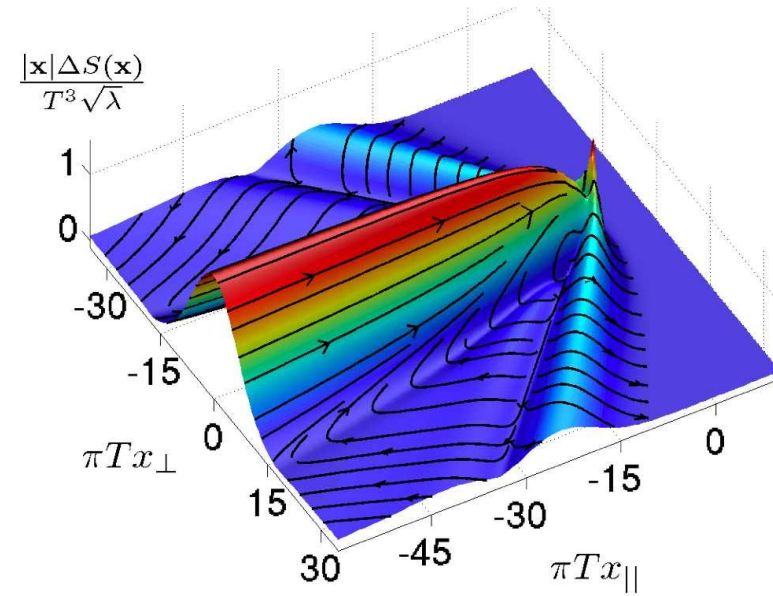
Beware of Jacobian amplified Beautiful Graphics

Jacobian $|x|$ amplified energy density and momentum density distributions

But the $O(N_c^2)$ background plasma signal is also Jacobian enhanced !



P. Chesler and L. Yaffe, PRD 78:045013 (2998)



$v=0.75$ string hologram

The question is what features survive thermal broadening after hadronization?

Chromo-Viscous hydrodynamics Neufeld(08), Asakawa et al (06) ... Heinz (86)

$$\partial_\mu \underset{\text{matter}}{T^{\mu\nu}} = \mathcal{S}^\nu = F^{\nu\alpha a} J_\alpha^a = \underset{\text{field}}{(F^{\nu\alpha a} \sigma_{\alpha\beta\gamma} * F^{\beta\gamma a})} \quad \text{Joule Heating}$$

$$T_{\text{tot}}^{\mu\nu}(X) = T_{bg}^{\mu\nu} + \delta T_{Mach}^{\mu\nu}(X) + \delta T_{Neck}^{\mu\nu}(X) + \delta T_{Coul}^{\mu\nu}(X) \quad \text{Total Stress}$$

The far zone $|x| \gg 1/3T$ can be approximated by Navier Stokes

$$\delta T_{Mach}^{\mu\nu}(X) = \left[sT \left(U^\mu U^\nu + \frac{3}{4} g^{\mu\nu} - \frac{\eta}{sT} \partial^{\{\mu} U^{\nu\}} \right) - T_{bg}^{\mu\nu} \right] \theta(1 - 3K_N)$$

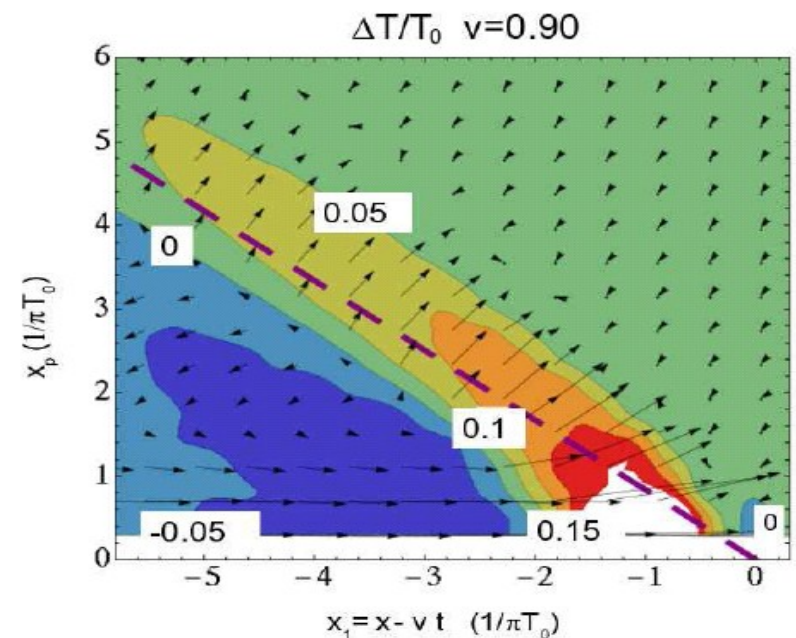
Knudsen Number $\sim \lambda(x)/L$

$$K_N(X) = \Gamma_s \frac{|\nabla \cdot \mathbf{M}|}{|\mathbf{M}|}$$

$$\Gamma_s \equiv 4\eta / (3sT) \geq 1 / (3\pi T)$$

Color Conductivity Selikhov, MG (93)

$$\sigma_{\mu\alpha\beta}(K) = ig^2 \int d^4P \frac{P_\mu P_\alpha \partial_\beta^P}{P \cdot K + i P \cdot U / \tau^*} f_0(P)$$



The relaxation or decoherence time τ^* is of the generic form noted in [23]

$$\frac{1}{\tau^*} = \frac{1}{\tau_p} + \frac{1}{\tau_c} + \frac{1}{\tau_{an}} \quad (7)$$

with $\tau_p \propto (\alpha_s^2 T \ln(1/\alpha_s))^{-1}$ being the collisional momentum relaxation time [13, 31], $\tau_c = (\alpha_s N_c T \ln(1/g))^{-1}$ being the color diffusion time defined in [30], and $\tau_{an} \propto (m_D(\eta|\nabla \cdot \mathbf{U}|/Ts)^{1/2})^{-1}$ being the anomalous strong electric and magnetic field relaxation time derived in Eq. (6.42) of [23]. Note that one can express

$$\tau_{an} \propto \frac{1}{gT} \frac{1}{\sqrt{K_N(X)}} \quad (8)$$

in terms of the local Knudsen number $K_N = \Gamma_s/L$ defined in Eq. (1) and used in Eq. (3). Here L is the characteristic stress gradient scale. However, because $\eta \propto \tau^* sT$, Eq. (8) is really an implicit equation for τ_{an} . Combining

these relations and taking into account the uncertainty principle constraint [13] that bounds $\tau^* \gtrsim 1/(3T)$ for an ultrarelativistic (conformal) plasma, we have

$$\frac{1}{\tau^*} \propto T \left(a_1 g^4 \ln g^{-1} + a_2 g^2 \ln g^{-1} + a_3 g \sqrt{K_N} \right) \lesssim 3T \quad (9)$$

where a_1, a_2, a_3 are numerical factors. As K_N gets large, τ_{an} can get small even in the weak coupling limit. Thus, large gradients, as in the near Neck zone, increase the importance of anomalous relaxation over color diffusion and collisional relaxation. Short relaxation times arise not only in strong coupling, such as in AdS/CFT, but also in pQCD in the presence of strong classical field gradients.

Magnitude of Joule Heating ($F^a J_a$) is determined by color conductivity

$$J_\nu^a(K) = \sigma_{\nu\mu\alpha}(K) F^{\mu\alpha a}(K)$$

$$\sigma_{\mu\alpha\beta}(K) = ig^2 \int d^4P \frac{P_\mu P_\alpha \partial_\beta^P}{P \cdot K + i P \cdot U / \tau^*} f_0(P) \quad (6)$$

where $f_0(P) = 2(N_c^2 - 1) G(P)$ is the effective plasma equilibrium distribution with $G(P) = (2\pi^3)^{-1} \theta(P_0) \delta(P^2) / (e^{-P \cdot U / T} - 1)$. Here, U^μ is the 4-velocity of the plasma

Long Wavelength: $U_\beta \sigma^{\mu\alpha\beta}(K \rightarrow 0) = -\tau^* m_D^2 g^{\mu\alpha} / 3$, where $m_D^2 = g^2 T^2$ is the Debye screening mass :

Since $\tau^* > 1/3T$, $\sigma(K=0) > g^2 T/9$

A very Subtle point: Only in Neck zone, $|x| < 1/3T = \lambda_T < \text{m.f.p.}$, BGNT08
are the relevant wavenumbers $K > 3T$ very large compared to $1/\tau^* \sim 3T$

$$\sigma_{\mu\alpha\beta}(K) = ig^2 \int d^4P \frac{P_\mu P_\alpha \partial_\beta^P}{P \cdot K + i P \cdot U / \tau^*} f_0(P)$$

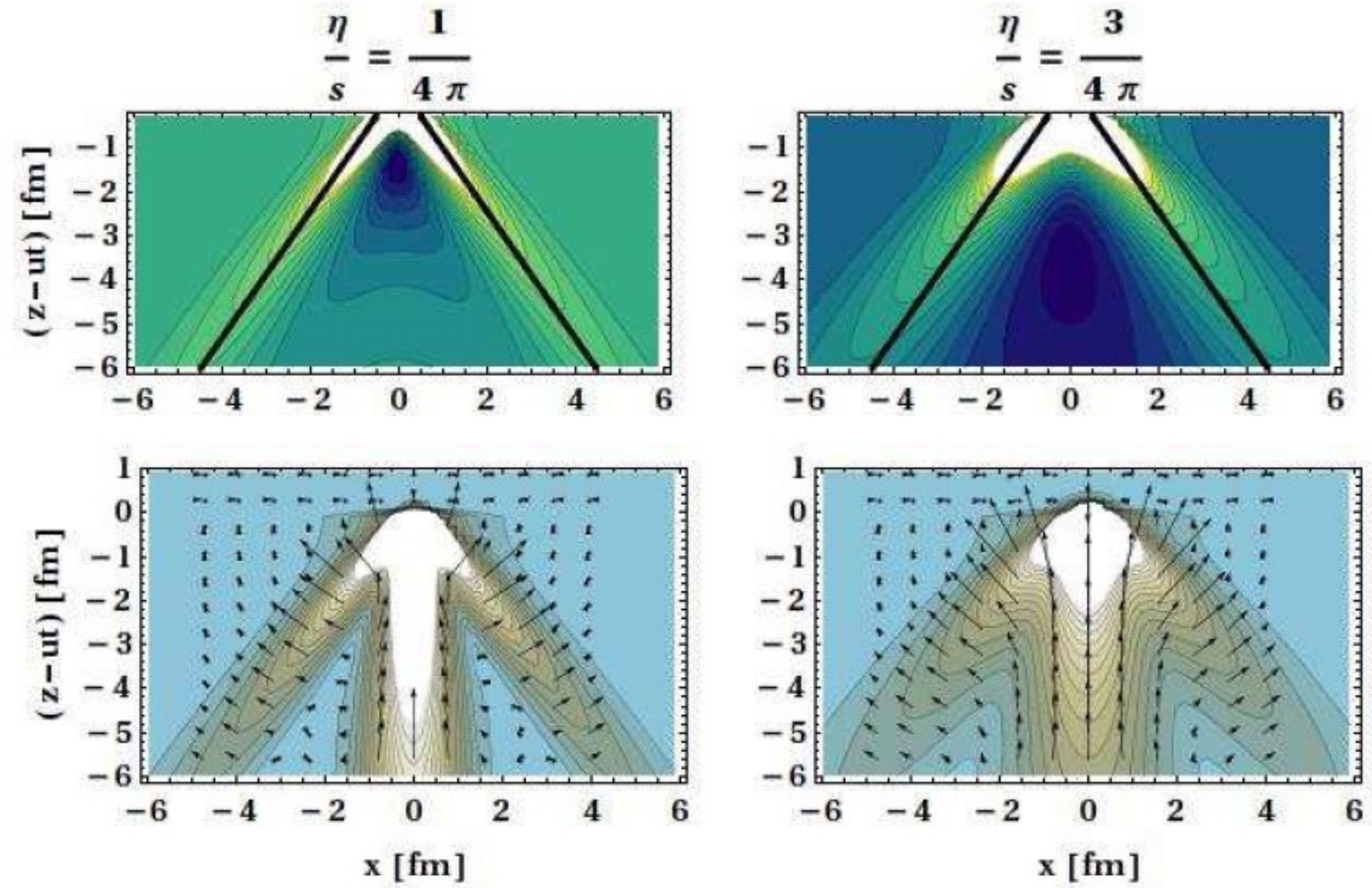
$$P \cdot K + i P \cdot U / \tau^* \xrightarrow{K \gg 3T} P \cdot K + i 0^+$$

Only in the Neck zone can we approximate
the high frequency conductivity neglecting the fast relaxation rate
i.e. $1/\tau^* \sim 0$ even as it reaches its maximum value, $3T$, in a sQGP !!

Neufeld, et al
Chromo-Hydro
with undamped
pQCD source

$$\partial_\mu T^{\mu 0} = \frac{\alpha_s (Q_p^a)^2 m_D^2}{8\pi(\rho^2 + \gamma^2 z_-^2)} \gamma u^2 \left(1 - \frac{\gamma u z_-}{\sqrt{z_-^2 \gamma^2 + \rho^2}} \right)$$

$$\partial_\mu T^{\mu i} = \frac{\alpha_s (Q_p^a)^2 m_D^2 u^2}{8\pi} \left(\frac{\gamma \mathbf{u}}{(z_-^2 \gamma^2 + \rho^2)^{3/2}} - \frac{u^2 (x, y, z_- \gamma^2)}{(z_-^2 \gamma^2 + \rho^2)^2} \right)$$



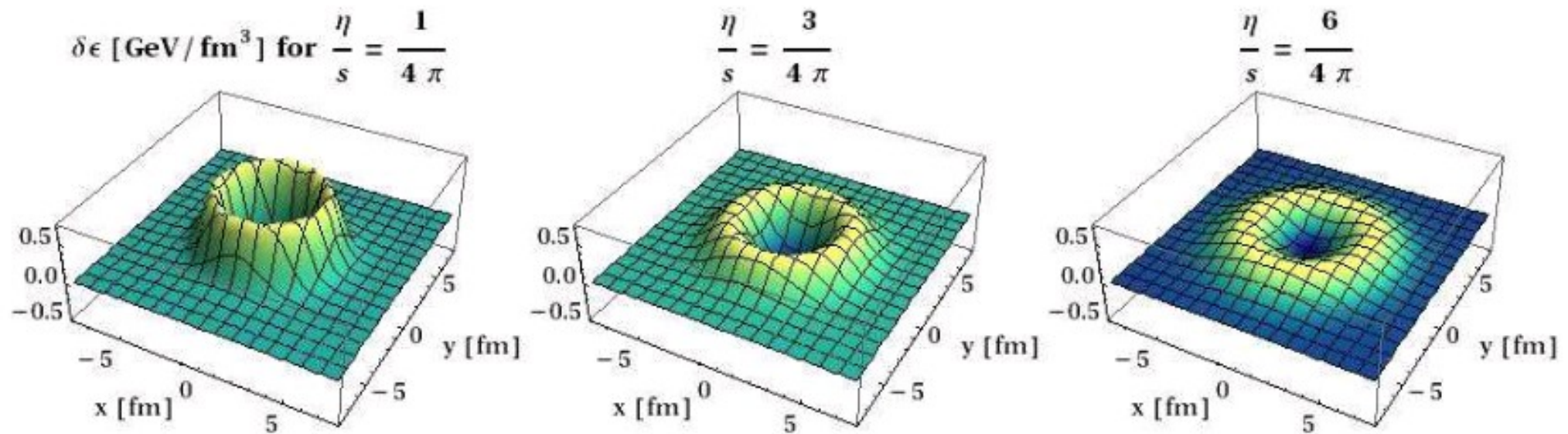


FIG. 3: (Color online) 3D plots of the perturbed energy density $\delta\epsilon(\mathbf{x}, t)$ in the $x-y$ plane at a distance of 4 fm behind the source gluon which moves in the positive z direction with $\gamma \approx 33$.

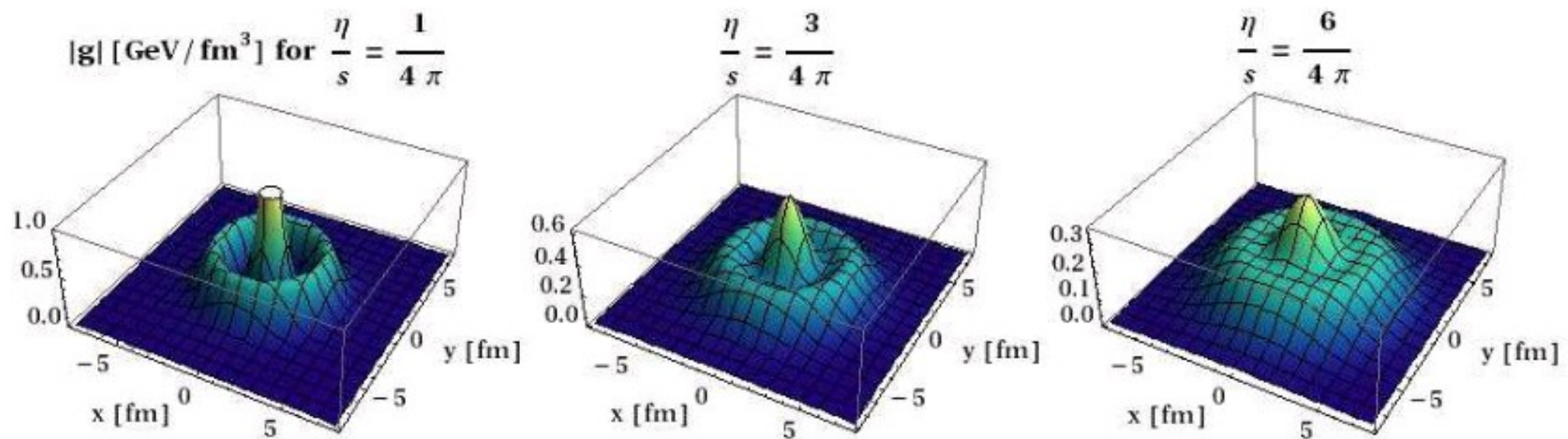


FIG. 4: (Color online) 3D plots of the magnitude of the perturbed momentum density, $|g| = |g_L(\mathbf{x}, t) + g_T(\mathbf{x}, t)|$ in the $x-y$ plane at a distance of 4 fm behind the source gluon, analogous to Figure 3

in our analysis. For associated (massless) particles with $P^\mu = (p_T, p_T \cos(\pi - \phi), p_T \sin(\pi - \phi), 0)$ the momentum distribution at mid rapidity $y = 0$ is

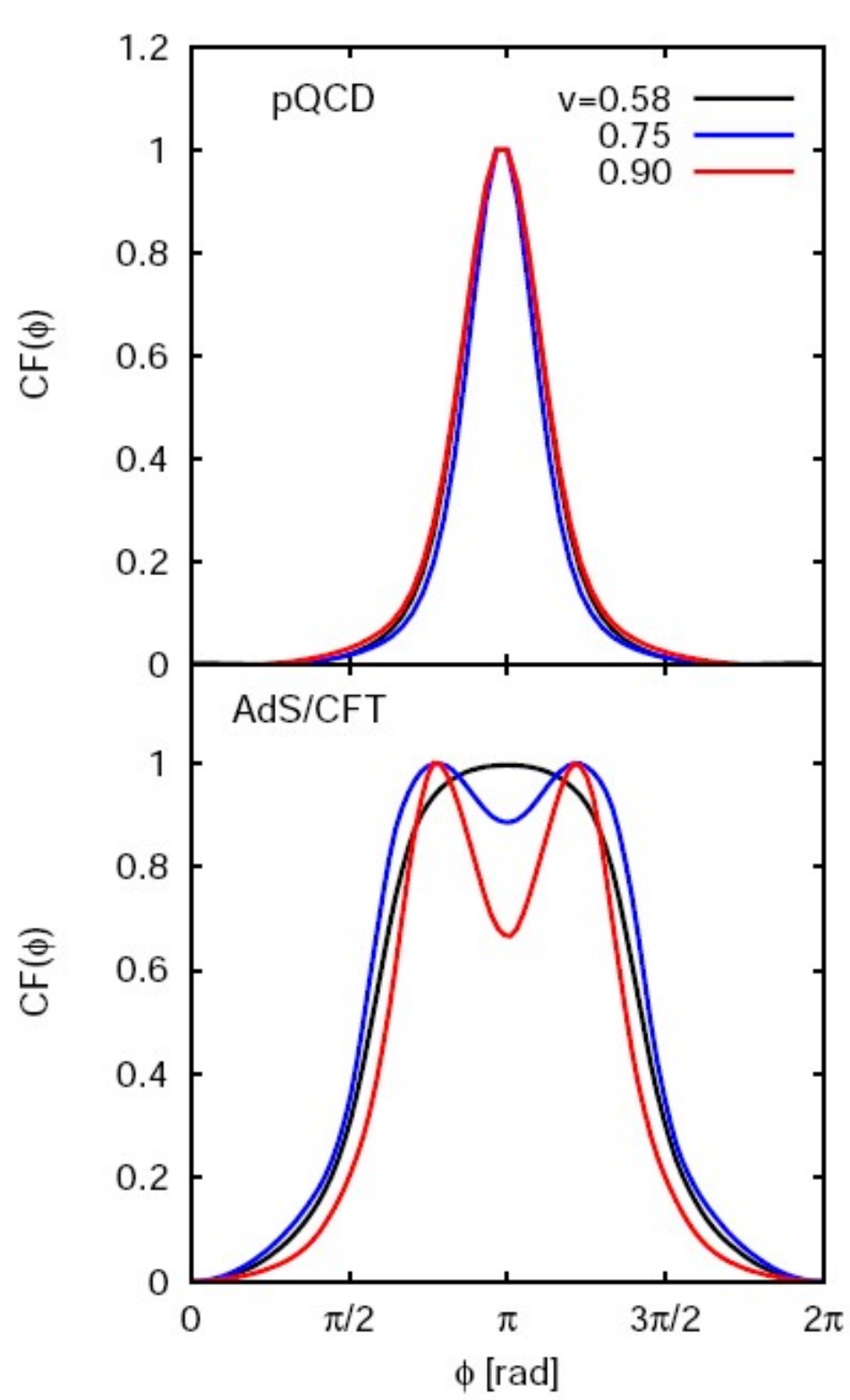
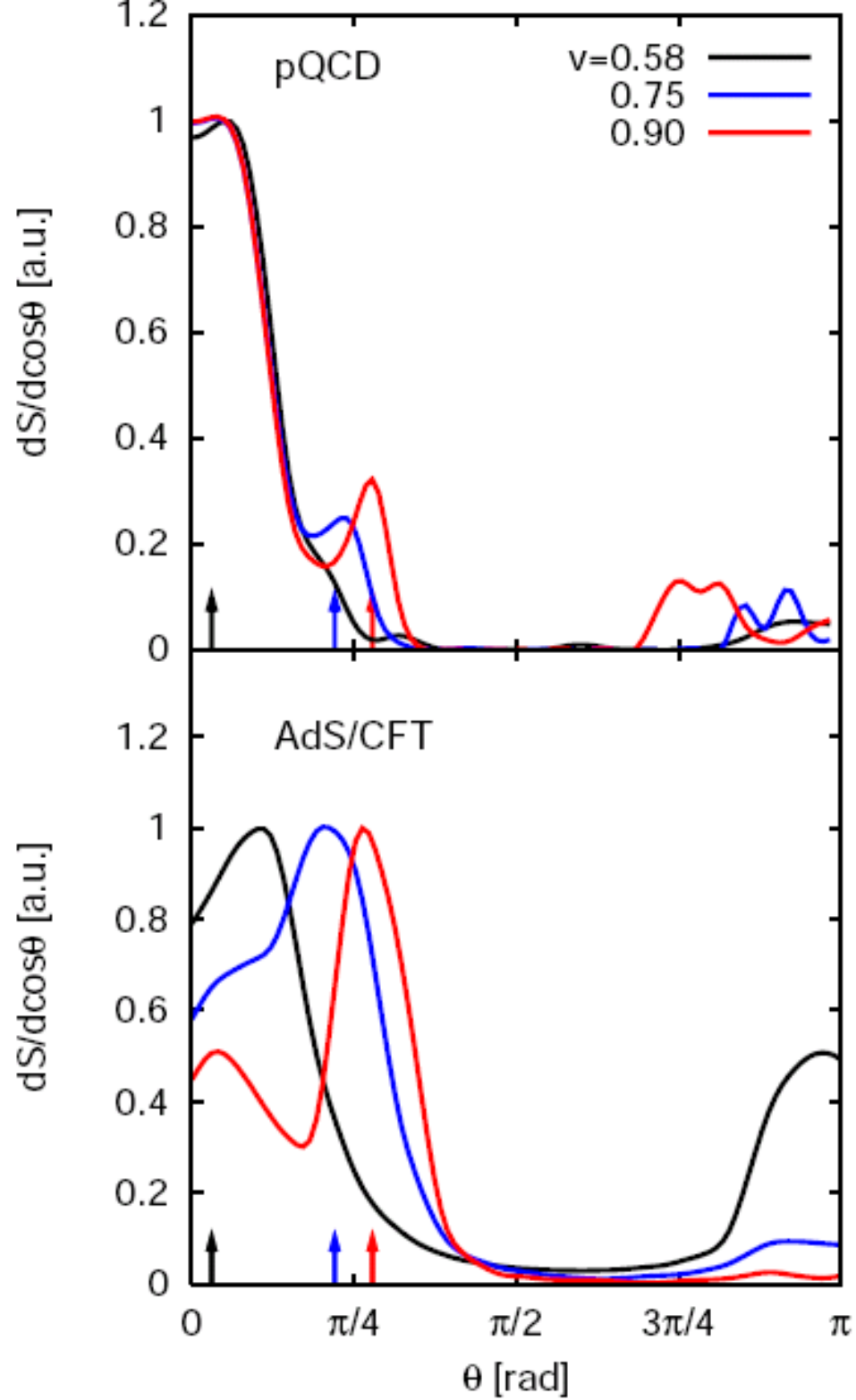
$$\left. \frac{dN}{p_T dp_T dy d\phi} \right|_{y=0} = \int_{\Sigma} d\Sigma_\mu P^\mu [f_0(U^\mu, P^\mu, T) - f_{eq}] \quad (10)$$

where p_T is the transverse momentum, $\Sigma(X)$ is the freeze-out hypersurface, and $f_0 = \exp(-U^\mu P_\mu / T(X))$ is a local Boltzmann equilibrium distribution. Viscous

As an independent calorimetric-like observable of collective flow we also investigate the bulk momentum weighted polar angle distribution (in the laboratory frame)

$$\frac{dS}{d \cos \theta} = \int d^3\mathbf{x} |\mathbf{M}(X)| \delta(\cos \theta - M_x(X)/|\mathbf{M}(X)|) \quad (11)$$

where $\theta = 0$ corresponds to the jet direction and $\theta \in [0, \pi]$. This quantity measures the total amount of mo-



Our results for the associated away side azimuthal distribution for $v = 0.58, 0.75, 0.90$ at mid-rapidity and $p_T = 12.5 T_0 = 2.5$ GeV in pQCD, computed using the output of the SHASTA code in Eq. (10), are shown in the upper panel of Fig. 4. We have defined the angular function

$$CF(\phi) = \frac{1}{N_{max}} \left(\frac{dN(\phi)}{p_T dp_T dy d\phi} - \frac{dN(0)}{p_T dp_T dy d\phi} \right) \Big|_{y=0} \quad (15)$$

where N_{max} is a constant used to normalize the plots.

My Summary (again):

This may be a smoking gun difference between wQGP pQCD quasiparticle transport and esQGP AdS string drag

What is the physics difference in these models?

In pQCD => Joule heating in the near ($r < 1$ fm) “Neck zone”

The very strong “Red Neck” physics predicted by AdS/CFT is still a mystery

Future identified heavy quark jet tomography will be decisive to judge between

Is the sQGP = $\lim_{\alpha \rightarrow 0.5}$ pQCD/wQGP ?

Is the sQGP = $\lim_{0.5 \leftarrow \alpha = \lambda/12\pi}$ BH/AdS drag ?

or something else ???

Gyulassy 10/10/08 BNL

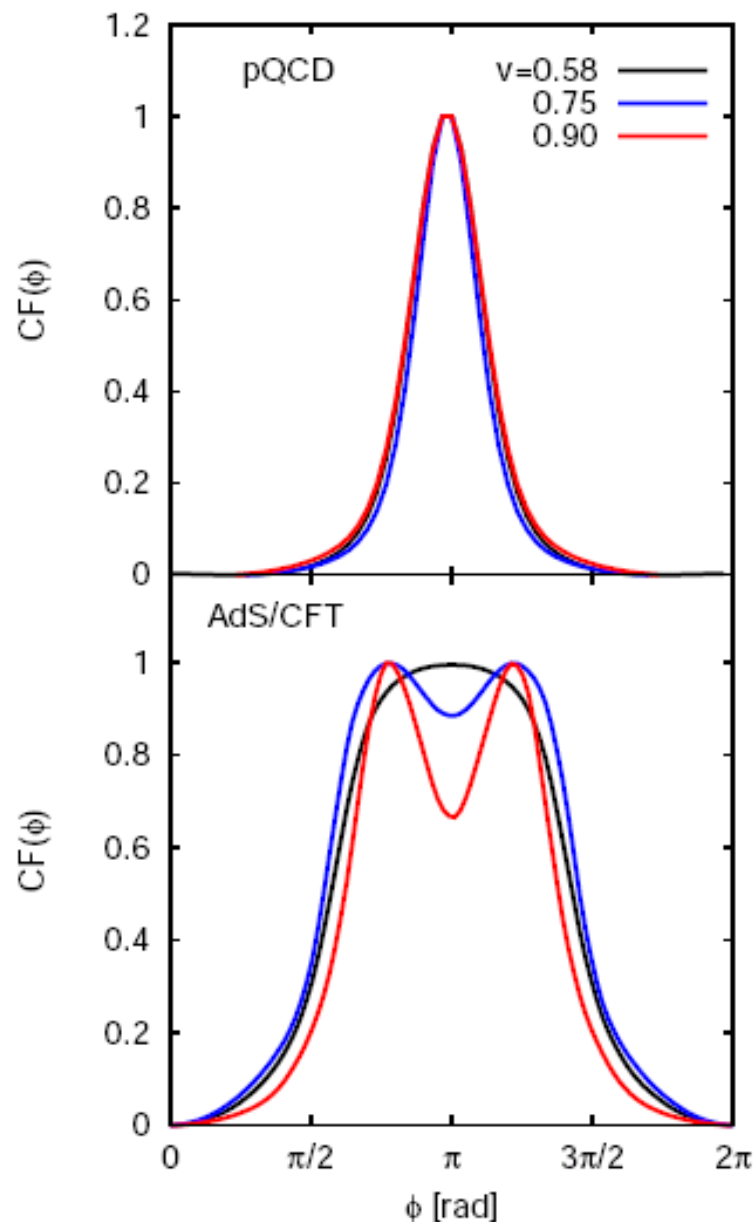
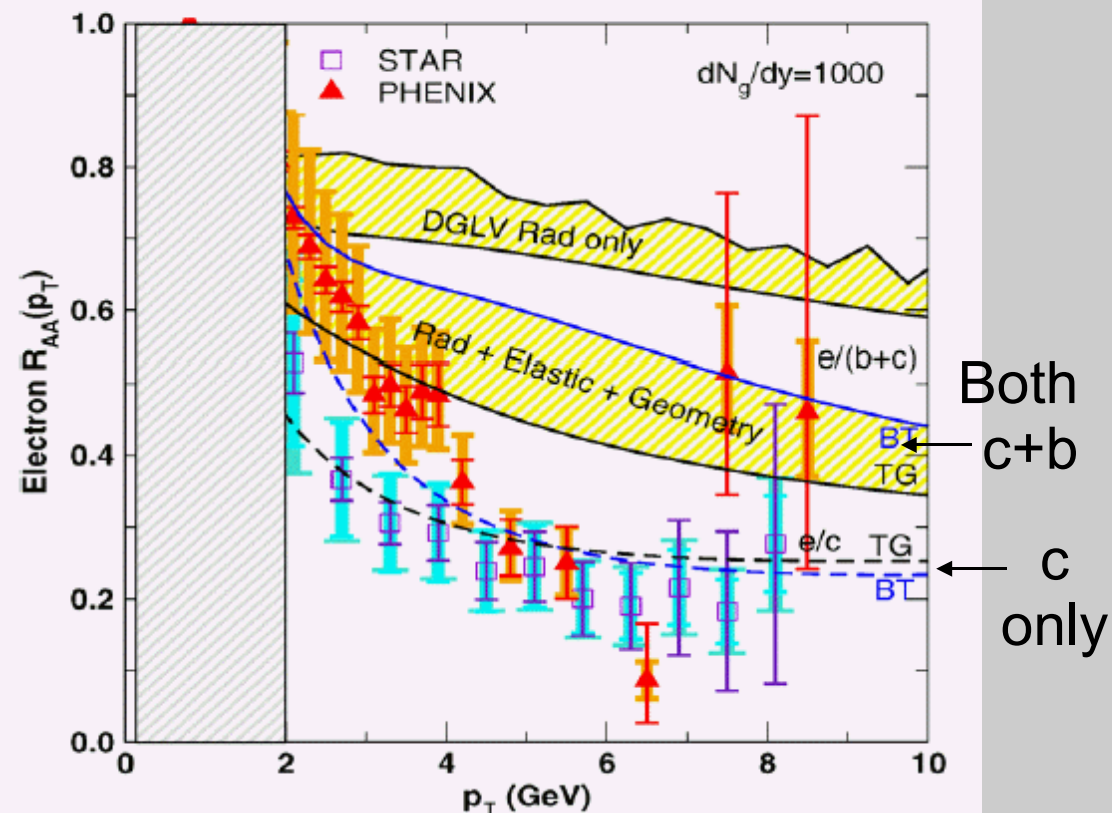
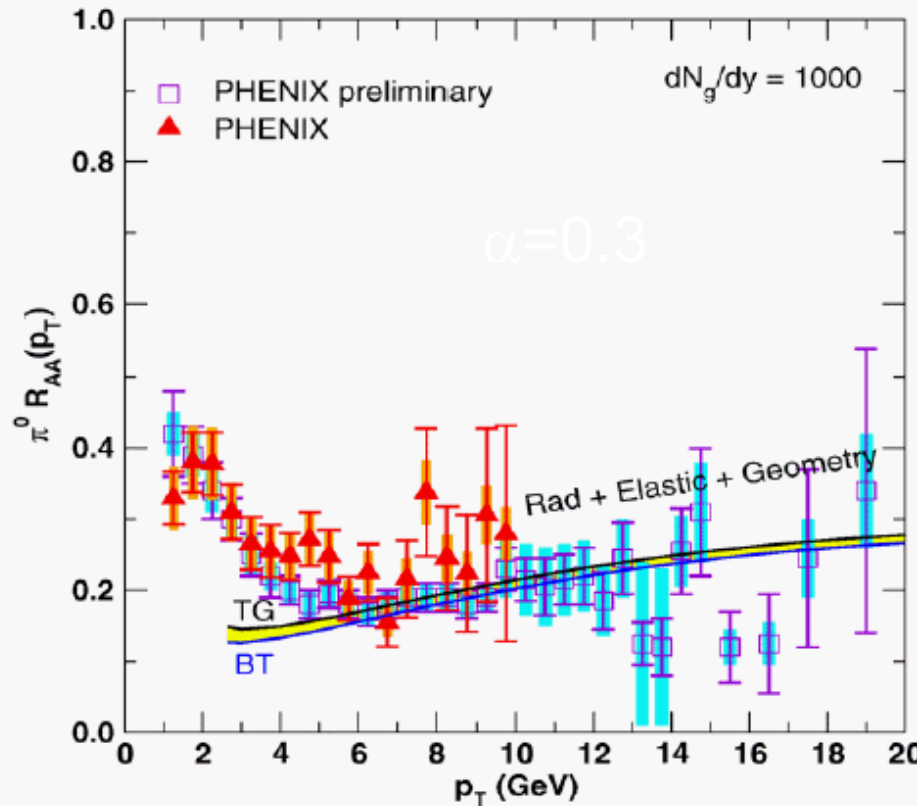


FIG. 4: (Color online) Normalized (and background subtracted) azimuthal away side jet associated correlation after Cooper-Frye freeze-out $CF(\phi)$ (see Eq. 15) for pQCD (top) and AdS/CFT from [5] (bottom). Here $CF(\phi)$ is evaluated at $p_T = 12.5 T_0 = 2.5$ GeV and $y = 0$. The black line is

Extra Slides

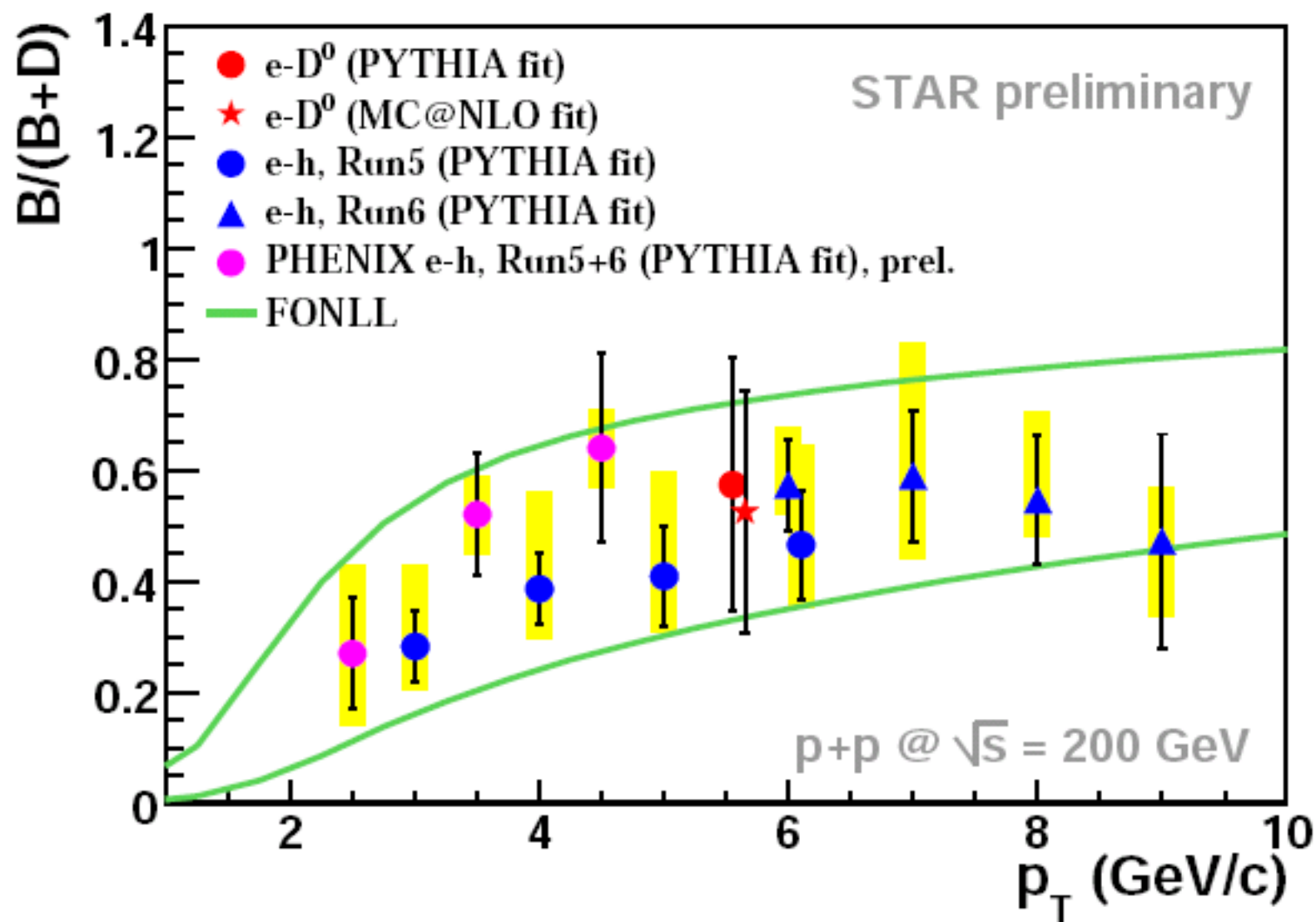
Current Light Quark vs Heavy Quark Jet Quenching Puzzle at RHIC

pQCD radiative energy loss explains light but fails for heavy
unless $\alpha \sim 0.5$ OR the Bottom drops out



Electron data seem to falsify pQCD HQ dynamics
unless Bottom quark production is suppressed
or $\alpha_s \rightarrow 0.5$ is moderately coupled

What is known about $b/(b+c)$ in elementary NN reactions at 200 AGeV



rapidity. Right panel of Fig. 1 shows the charm cross section as a function of rapidity compared to theoretical calculations [18], the clear difference is seen between STAR and PHENIX results at mid-rapidity with systematical errors dominated. PHENIX also obtained the charm cross section from muon measurement at forward rapidity ($\langle y \rangle = 1.65$, $1.0 \leq p_T \leq 3.0$ GeV/c) in 200 GeV $p + p$ collisions, shown as the triangles. The new result has smaller systematical error and consistent with theory curves [15].

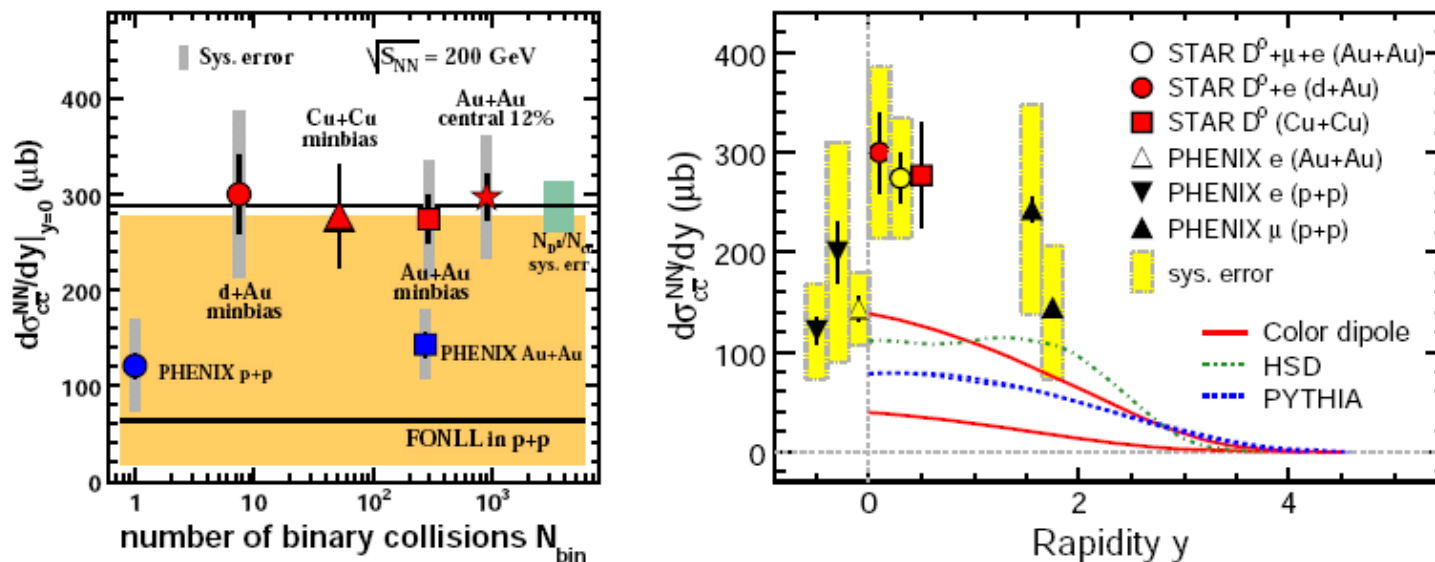


Figure 1. Panel (a): Mid-rapidity charm cross section per nucleon-nucleon collision as a function of N_{bin} in $d+Au$, minbias and 0–12% central $Au+Au$ collisions. The solid line indicates the average. FONLL prediction is shown as a band around the central value (thick line) [17].

Jiang-yong Jia Int.J.Mod.Phys.E16:3058,2008

1) Two component Model $C^{AB}(\Delta\phi) = a_o[C_H^{AB}(\Delta\phi) + J(\Delta\phi)]$

2) ZYAM?: $C^{AB}(\phi_{\min})=0$ $C_H^{AB}(\Delta\phi) = [1 + 2v_2 \cos 2(\Delta\phi)]$; $v_2 = (v_2^A \times v_2^B)$

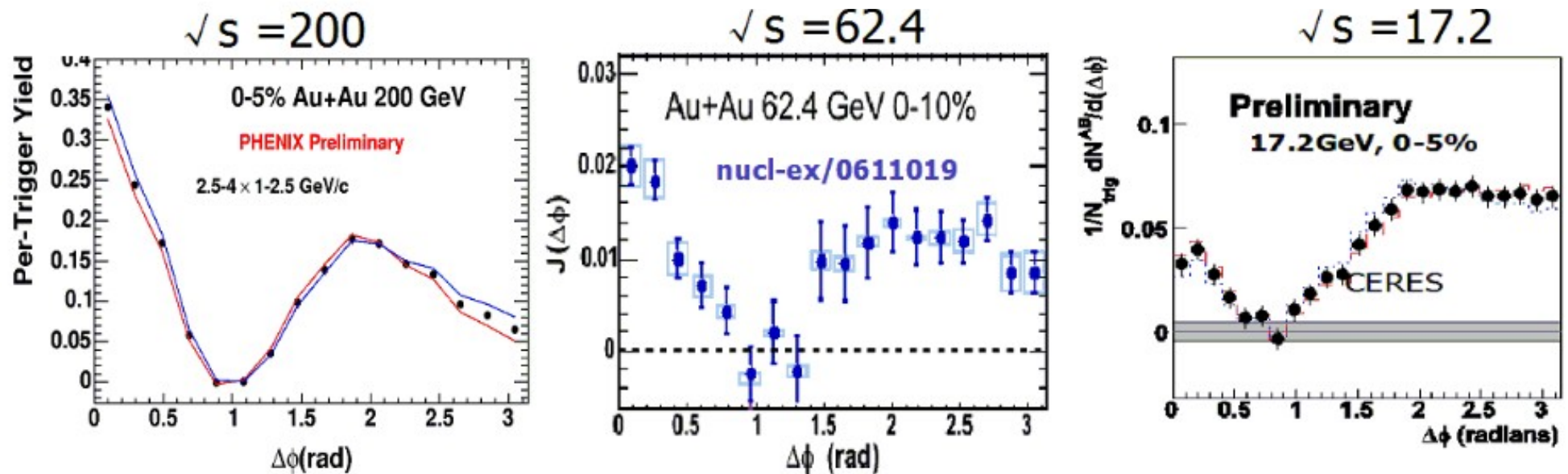


Fig. 7. a) Per-trigger yield in central Au+Au collisions at $\sqrt{s_{NN}} = 200$ GeV from PHENIX. b) The extract jet function at $\sqrt{s_{NN}} = 62.4$ GeV from PHENIX. c) Per-trigger yield at $\sqrt{s_{NN}} = 17.3$ GeV from CERES.

[MG] Why is broad away side correlation so weakly dependent on beam energy?

2. Bulk elliptic flow is much less perfect at SPS

3. True high pT pQCD power law jet physics is suppressed at SPS kinematics

4. The minijet $p_t < 3$ GeV range is swamped by non-jet semi-soft coalescence

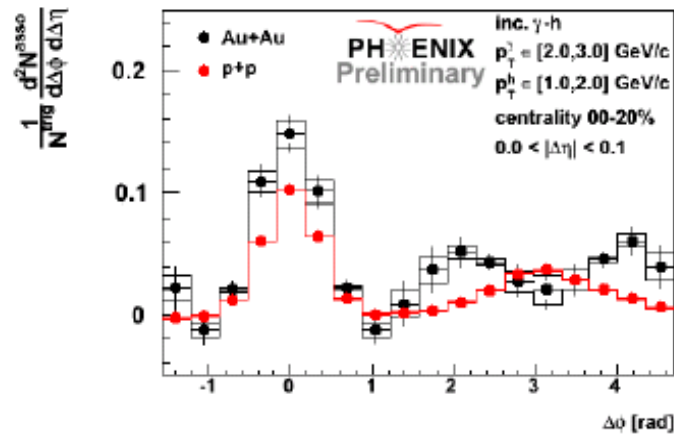


Fig. 1. $\Delta\phi$ distributions of correlated inclusive photon-hadron pairs in central Au+Au collisions (black) and p+p collisions (red). The photons have $2.0 < p_T < 3.0$ GeV/c and the hadrons have $1.0 < p_T < 2.0$ GeV/c. From Ref. [5].

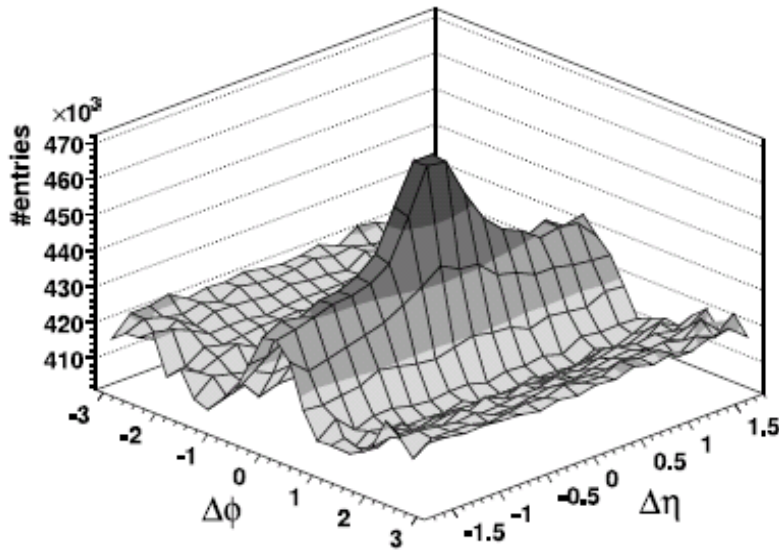


Fig. 2. $\Delta\phi$ v. $\Delta\eta$ distributions of correlated hadron pairs in central Au+Au collisions. Triggers have $3.0 < p_T < 4.0$ GeV/c and associated particles have $2.0 < p_T < p_{T, \text{trig}}$. From Ref. [6].

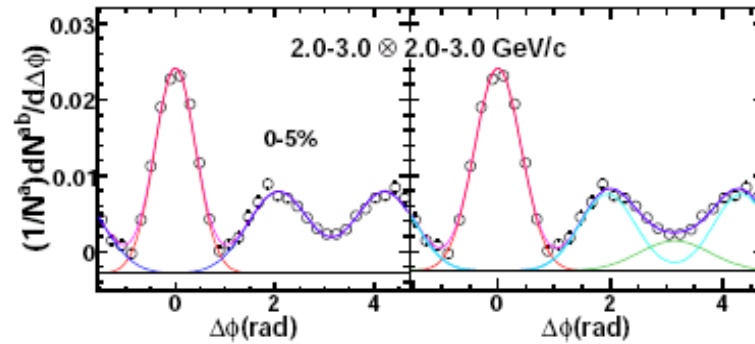


Fig. 3. Fits to distributions of correlated hadrons. The left panel shows the away side described by a two Gaussian fit and the right panel shows the away side described by a three Gaussian fit with the additional Gaussian centered at $\Delta\phi = \pi$. Both fits describe the data relatively well. From Ref. [4].

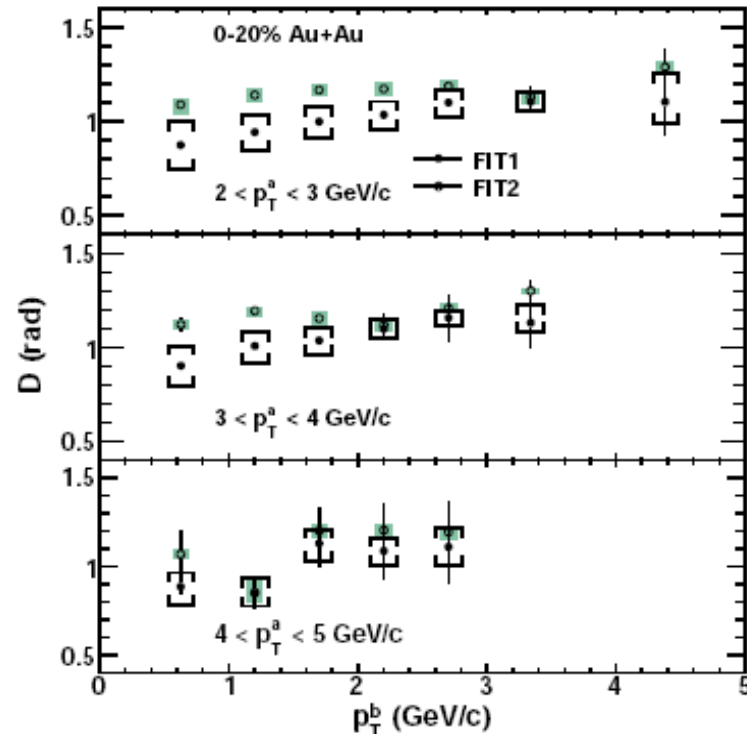


Fig. 4. D extracted with two-Gaussian (solid points) and three-Gaussian (hollow points) fit from correlations between

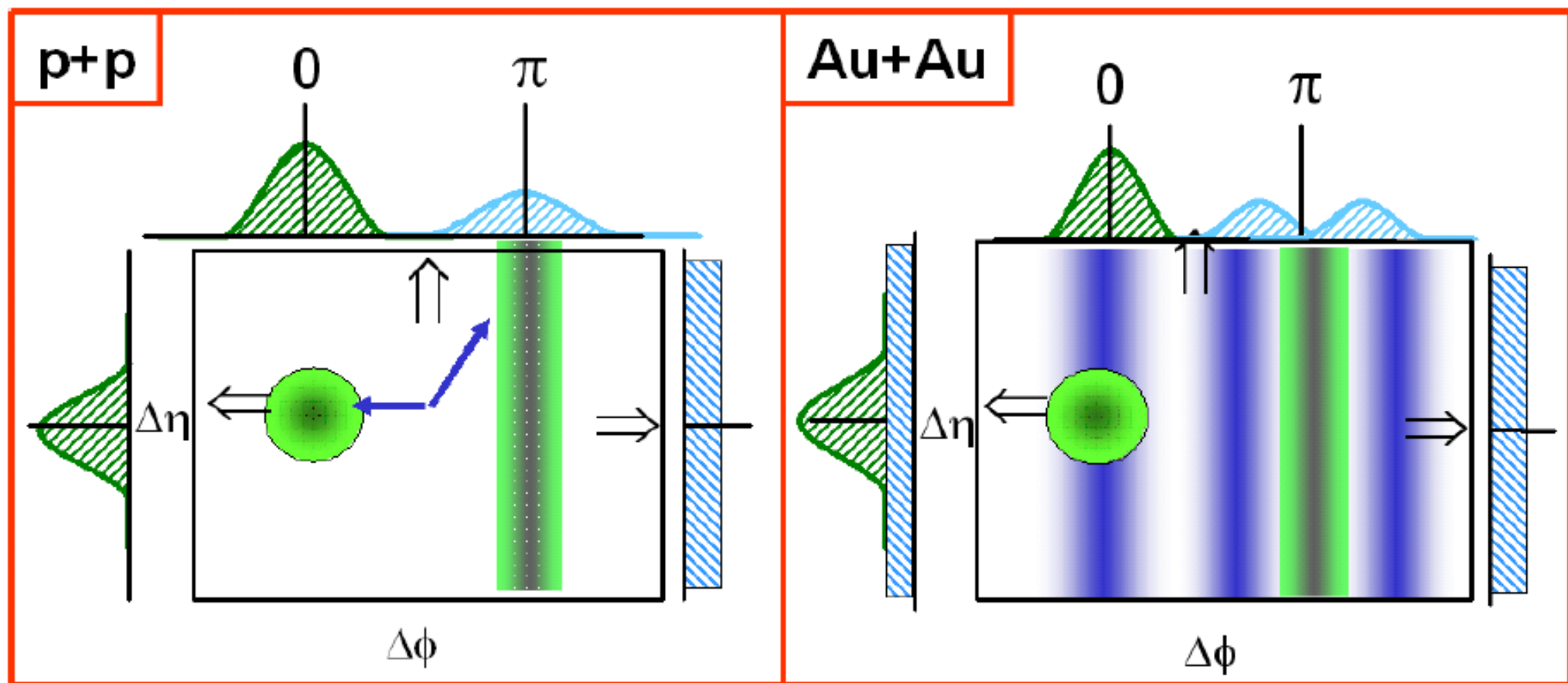


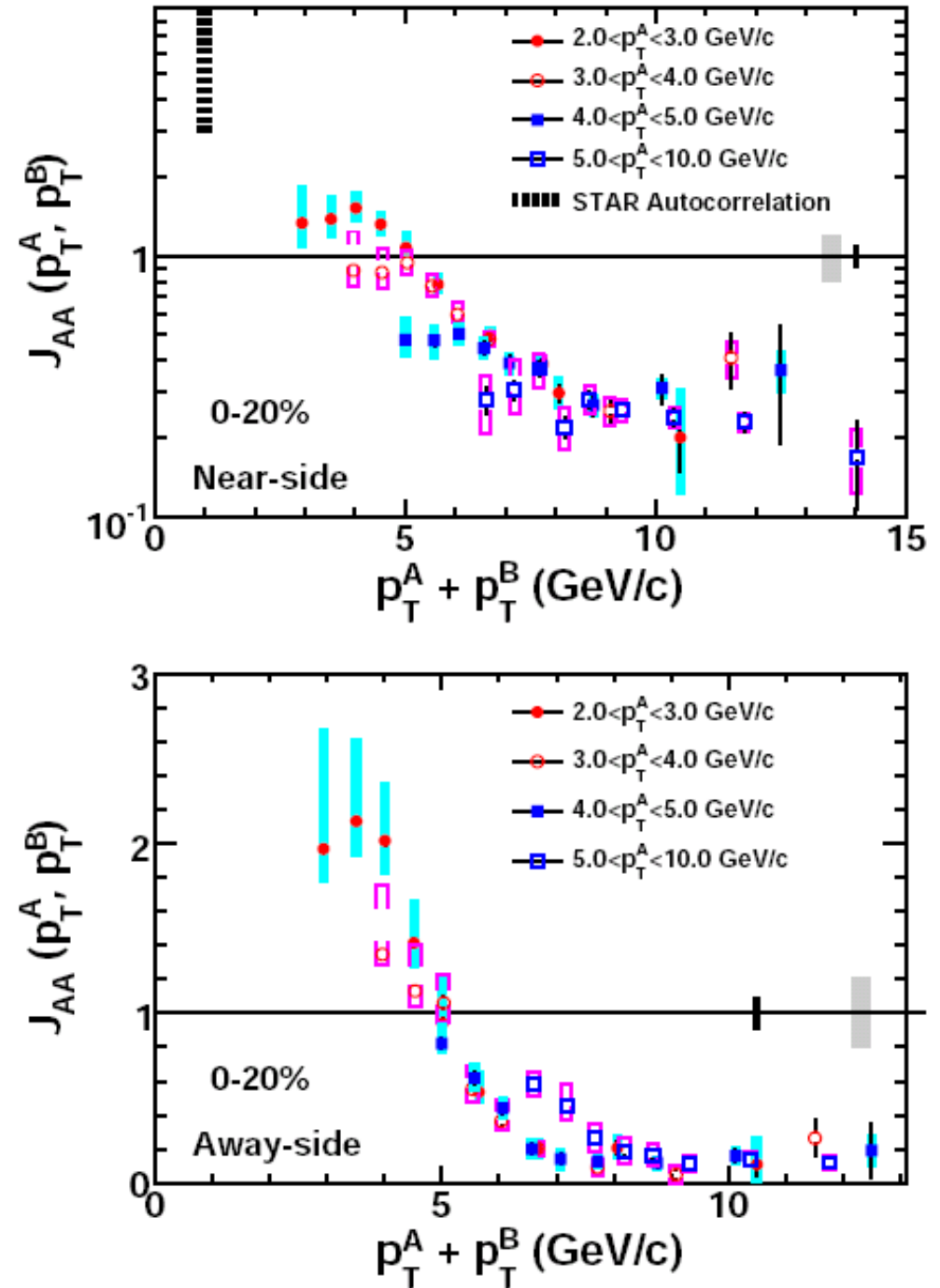
Fig. 1. A schematic illustration of the jet-induced di-hadron correlation signal in $\Delta\phi$ and $\Delta\eta$ and associated projections in $\Delta\phi$ or $\Delta\eta$ for (left) $p + p$ and (right) central Au+Au collisions. The medium response components in Au+Au is illustrated by fuzzy blue band.

The modification of pair yield in Au+Au collision can be characterized by J_{AA} :

$$J_{AA}(p_T^a, p_T^b, \Delta\phi) = \frac{JPY^{A+A}}{\langle N_{coll} \rangle JPY^{p+p}} \quad (1)$$

$$= \frac{1}{\sigma_{A+A}} \frac{d^3\sigma_{jet_ind}^{A+A}}{dp_T^a dp_T^b d\Delta\phi} \bigg/ \frac{\langle N_{coll} \rangle}{\sigma_{p+p}} \frac{d^3\sigma_{jet_ind}^{p+p}}{dp_T^a dp_T^b d\Delta\phi}$$

J_{AA} quantify the medium modification of hadron pair yield from the expected yield, in a way similar to R_{AA} for describing the modification of single hadron yield. The hadron pair yield is proportional to the di-jet yield, and in the absence of nuclear effects, it should scale with N_{coll} and $J_{AA} = 1$. Fig. 6 shows J_{AA} as a function of pair proxy energy ($p_T^{sum} = p_T^A + p_T^B$) for the near- (top panel) and away-side (bottom panel). In contrast to a constant suppression at large p_T^{sum} , the pair yields are less suppressed at $p_T^{sum} < 6 - 8$ GeV/c. This reflects directly the energy transport that redistributes energy of the quenched jets to low p_T hadrons (i.e. medium response). We would like to



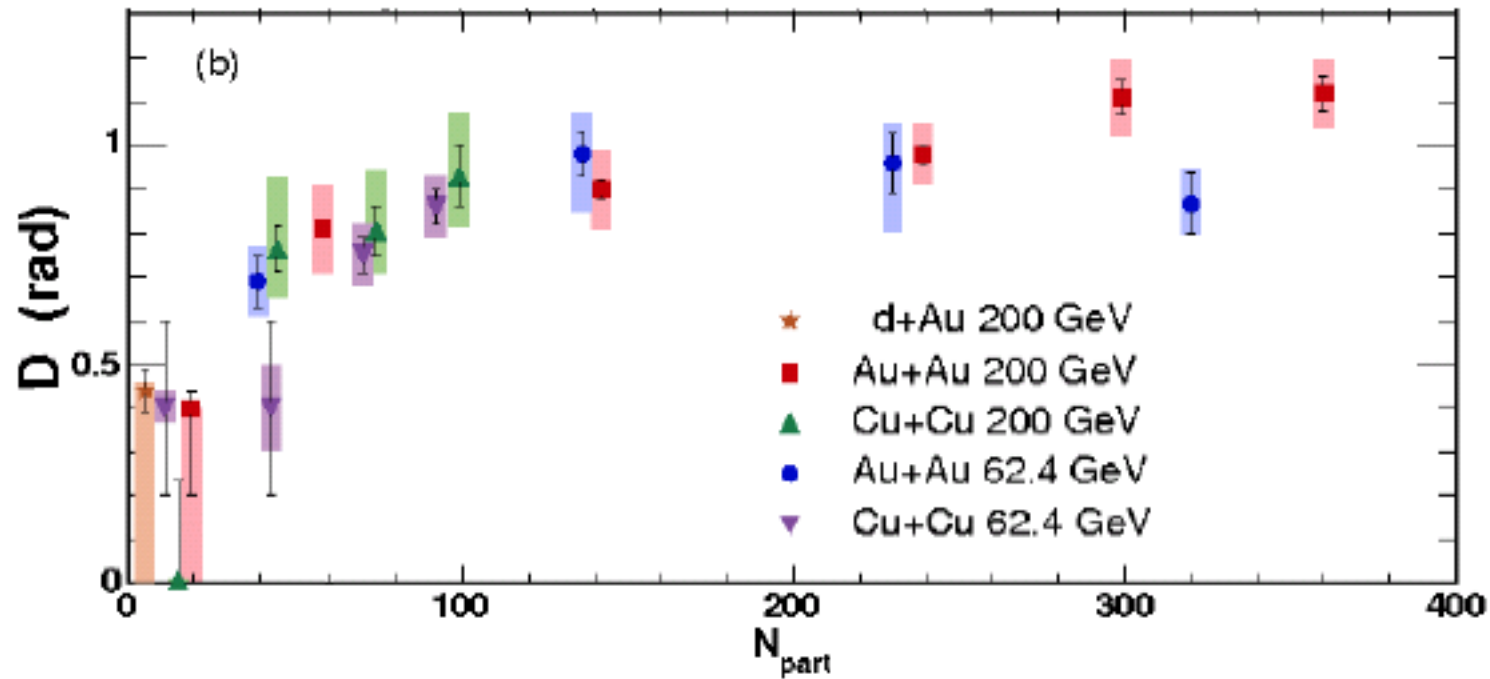


Fig. 5. D extracted with a two-Gaussian fit from correlations between hadron pairs with triggers at $2.5 < p_T < 4.0 \text{ GeV}/c$ and associated particles with $1.0 < p_T < 2.5 \text{ GeV}/c$. From Ref. [9].